Vectorisation of residual gravity and TMI data in the northern Gawler Craton: Implications for exploration targeting and GIS analysis

Laszlo F Katona, Tom Wise and Anthony Reid

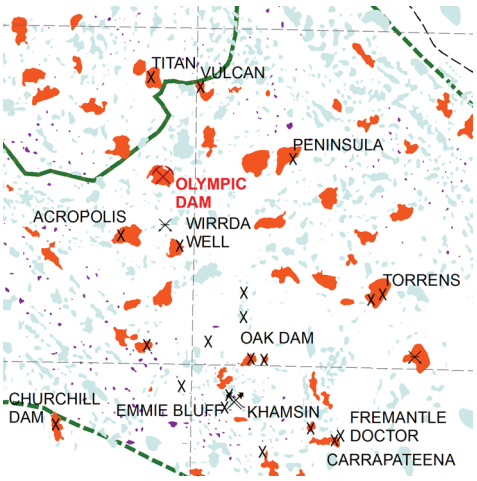

Report Book
2016/00037

SOUTH AUSTRALIA

Government of South Australia
Department for Energy and Mining

Vectorisation of residual gravity and TMI data in the northern Gawler Craton: Implications for exploration targeting and GIS analysis

Laszlo F Katona, Tom Wise and Anthony Reid

Geological Survey of South Australia
Department for Energy and Mining

July 2018

Report Book 2016/00037

Department for Energy and Mining
Level 7, 101 Grenfell Street, Adelaide
GPO Box 320, Adelaide SA 5001
Phone +61 8 8463 3037
Email dem.minerals@sa.gov.au
www.energymining.sa.gov.au

South Australian Resources Information Gateway (SARIG)
SARIG provides up-to-date views of mineral, petroleum and geothermal tenements and other geoscientific data. You can search, view and download information relating to minerals and mining in South Australia including tenement details, mines and mineral deposits, geological and geophysical data, publications and reports (including company reports).
map.sarig.sa.gov.au

Preferred way to cite this publication
Katona LF, Wise T and Reid A 2018. *Vectorisation of residual gravity and TMI data in the northern Gawler Craton: Implications for exploration targeting and GIS analysis*, Report Book 2016/00037. Department for Energy and Mining, South Australia, Adelaide.

CONTENTS

ABSTRACT **1**

AIMS AND INTRODUCTION **1**

GEOLOGICAL SETTING **2**

METHOD **3**

INPUT GRIDS 3
GRID PREPARATION (GRAVITY) 4
GRID PREPARATION (TMI) 5
DELINEATION OF GEOPHYSICAL HIGHS FROM EACH GRID, USING A GEOPROCESSING SCRIPT (ARCGIS), APPLIED TO $OUTPUTGRID_{RESIDUAL}$ 6
DATASET CHECKS AND MANUAL CLEAN-UP 8
DATA CLASSIFICATION AND CLUSTER MAPPING 9

RESULTS **9**

GRAVITY DATA 9
TMI DATA 14
CONTOUR DATASETS 17
COINCIDENT ANOMALIES 17

DISCUSSION **19**

RATIONALE 19
TECHNIQUE TO GENERATE A RESIDUAL FIELD 19
ZONAL STATISTICS ATTRIBUTES 19
EXAMPLES OF HIGH VALUES IN THE GRAVITY DATASET 21
CLUSTERING OF HIGH MAGNITUDE RESIDUAL GRAVITY ANOMALIES 21
EXAMPLES OF HIGH VALUES IN THE TMI DATASET 22
CLUSTERING OF HIGH MAGNITUDE RESIDUAL TMI ANOMALIES 22
EVALUATING SPATIALLY COINCIDENT GRAVITY AND TMI ANOMALIES 24

FUTURE WORK **25**

THE DATA PACKAGE **25**

ACKNOWLEDGEMENTS **25**

REFERENCES **25**

APPENDIXES **27**

APPENDIX 1. DATA PACKAGE CONTENTS – GRID DATASETS 27
Gravity 27
APPENDIX 2. DATA PACKAGE CONTENTS – VECTOR DATASETS 31
Gravity 31
TMI 33
APPENDIX 3. DATA PACKAGE METADATA 36

TABLES

Table 1. Gravity and TMI grids, extents and cell size used in the analysis. 3
Table 2. Excerpt from the attribute table for magnetic anomalies polygon dataset displaying zonal statistics: minimum (RES_MIN), maximum (RES_MAX), mean (RES_MN), standard deviation (RES_STD), count of cells within each polygon (RES_CNT), sum of cells within each polygon (RES_SUM), range (RES_RNG), and Magnitude (calculated by subtracting Contour from MAX). 8
Table 3. High and low values of polygon attributes for residual gravity. 11
Table 4. High and low values of polygon attributes for residual TMI. 14

FIGURES

Figure 1. Location of the study area showing the extent of reprocessed gravity and magnetic data overlaying Archean-Mesoproterozoic solid geology of the Northern Gawler Craton, shaded by total magnetic intensity sunshade image. Geophysical domains and summary geology of the central-northern Gawler Craton are also shown. Abbreviations: MCR = Mabel Creek Ridge, CPR = Coober Pedy Ridge, MWD = Mount Woods Domain, PDI = Peake and Denison Inliers, HGB = Harris Greenstone Belt. (Plan number 205084-001) 2
Figure 2. Subset region within the study area, displaying gravity (a) and gravity upward continued 1000 m (b). The upward continued gravity is a smoother image with less detail, representative of the response from deep sources. 4
Figure 3. The same subset region within the study as that shown in Figure 2, displaying residual gravity (Gravity – Gravity upward continued 1000 m). The residual grid attenuates deeper sources and intensifies features thought to be nearer the surface. 4
Figure 4. Subset region within the study area, displaying reduced to pole TMI (a) and Reduced to pole TMI upward continued 1000 m (b). 5
Figure 5. The same subset region within the study as that shown in Figure 4, displaying residual TMI (Reduced to pole TMI – Reduced to pole TMI upward continued 1000 m). 5
Figure 6. TMI contours up to 60 km in length (a) and gravity contours up to 30 km in length (b). Note: the density of the gravity contours (0.1 mGal contour interval) makes them appear as solid objects. 7
Figure 7. Anomalies outlined by polygons whose centroid value exceeds the perimeter value; TMI (a) and gravity (b). 7
Figure 8. Centroids of grid cells are shown intersecting an anomaly polygon. The grid cells of intersected centroids are used in the statistical calculations for each feature. RES_CNT for this feature is 41. 7
Figure 9. TMI dataset checking and correction. (a) illustrates the issue of an anomaly not selected by the automated routine due to central low in the TMI feature at the centre of the figure; (b) anomaly subsequently delineated and appended by selecting and polygonising the appropriate contour from the contour dataset generated by the geoprocessing routine. 8
Figure 10. Residual gravity anomaly polygons symbolised by anomaly magnitude (MAX – Contour). Warmer colours indicate high magnitude anomalies. High magnitude anomalies appear to spatially cluster. (Plan number 205084-002) 10
Figure 11. A gravity station density grid broadly corresponds with a higher number of delineated anomalies per unit area. 10
Figure 12. The Wilgena Hill iron ore deposit has the highest anomaly magnitude recorded by the anomaly processing routine at 48.5 mGals. 11
Figure 13. The Peculiar Knob iron ore mine has the highest anomaly maximum recorded by the anomaly processing routine at 97.8 mGals and the highest mean value at 77.7 mGals. 12
Figure 14. The figure is generated by the ArcGIS High/Low clustering (Getis-Ord General G) tool and demonstrates the output of the Getis-Ord General G analysis. The z-score of 13.099757 indicates high magnitude gravity anomaly clustering across the study area is non-random. 13

Figure 15. The cluster outlier analysis of gravity anomaly magnitude reveals clustering of high magnitude anomalies over the Coober Pedy Ridge, Mabel Creek Ridge, Mount Woods Domain and Peake and Denison Inliers. High-low clusters (outlier anomalies) are evident in the Eastern Gawler Province. The red line delineates the extent of a region of high-low clusters covering the Olympic Domain. (Plan number 205084-003) 13
Figure 16. Residual RTP TMI anomaly polygons symbolised by anomaly magnitude (MAX – Contour). Warmer colours are indicative of high magnitude anomalies. (Plan number 205084-004) 14
Figure 17. The Giffen Well deposit has the highest anomaly magnitude and maximum recorded by the anomaly processing routine at 18520 nT. 15
Figure 18. The Getis-Ord General G statistic is used to determine if apparent clustering of high or low magnitude magnetic anomalies is the result of random chance. The z-score of 5.29 indicates significant, non-random high clusters. The figure is generated by the ArcGIS High/Low clustering tool. 15
Figure 19. The cluster analysis of TMI anomaly magnitude reveals clustering of high magnitude anomalies over Coober Pedy Ridge, Mabel Creek Ridge, Mount Woods Domain, Peake and Denison Inliers, Wilgena Domain, Fowler Domain and the Harris Greenstone Belt. High-low clusters occur mainly across the southern half of the study area. Abbreviations: MCR = Mabel Creek Ridge, CPR = Coober Pedy Ridge, MWD = Mount Woods Domain, PDI = Peake and Denison Inliers, HGB = Harris Greenstone Belt. (Plan number 205084-005) 16
Figure 20. Contours within gravity anomalies provide an indication of the distribution of residual gravity within anomalous regions. 17
Figure 21. Spatially coincident gravity and TMI anomalies. In this example 1000 m lateral separation is considered coincident, resulting in 8856 TMI polygons and 4259 gravity polygons. (Plan number 205084-006) 18
Figure 22. Spatially coincident gravity and TMI anomalies. In this example 100 m lateral separation is considered coincident resulting in 5705 TMI polygons and 3524 gravity polygons. (Plan number 205084-007) 18
Figure 23. A reversely magnetised region within an anomaly produces a magnetic minimum that is lower than the value of the contour at the perimeter of the anomaly. 20
Figure 24. Filtered residual RTP TMI anomalies with a magnitude greater than 1000nT. The magnitude is the calculated difference between the contour value defining an anomaly and maximum value within the anomaly. (Plan number 205084-008) 20
Figure 25. High-low clustering of gravity anomalies within the Olympic Domain coincide with known IOCG deposits and occurrences, including Olympic Dam. The green lines show the informal Olympic Subdomain and Undifferentiated Precambrian domain boundaries. (Plan number 205084-009) 22
Figure 26. Low to moderate magnitude TMI anomalies in the Olympic domain coincident with high magnitude gravity anomalies in the Olympic Domain. 23
Figure 27. Low to moderate magnitude TMI anomalies in the Olympic domain coincident with high magnitude gravity anomalies in the Olympic Domain. 24

Vectorisation of residual gravity and TMI data in the northern Gawler Craton: Implications for exploration targeting and GIS analysis

Laszlo F Katona, Tom Wise and Anthony Reid

ABSTRACT

Gravity and reduced-to-pole total magnetic intensity grids over the northern Gawler Craton have been vectorised, generating polygon datasets representing regions of locally anomalous gravity and magnetic intensity. Statistics from potential field grids were embedded into each polygon which enabled calculation of anomaly magnitude. Known IOCG-type deposits were found to be consistently associated with coincident to semi-coincident magnetic and gravity anomalies, with residual Bouguer gravity anomaly magnitudes greater than 4.8 milliGals (mGal). Known iron ore deposits were found to be associated with residual TMI anomaly magnitudes greater than 3800 nanoTesla (nT). Analysis of spatial clustering and the identification of outliers using Anselin Local Morans I (ESRI, 2013) has resulted in the delineation of geographic regions across the study area that exhibit either high magnitude clusters or high magnitude outliers, which correspond to known regional geological and metamorphic domains. In the eastern Gawler Craton, high magnitude spatial outliers are of particular interest, as they include a high proportion of currently identified iron oxide – copper–gold (IOCG) deposits and mineral occurrences. Moreover, these spatial outliers appear to lie within the Olympic Domain, possible re-defining the extent of the domain. Results from this study suggest additional untested spatially coincident magnetic and gravity anomalies that warrant further investigation.

AIMS AND INTRODUCTION

Geophysical targeting methods using gravity and total magnetic intensity (TMI) images have been widely used by explorers as targeting criteria for a range of commodities. The aim of this report is to outline and discuss a methodology for the vectorisation and attribution of potential field gravity and magnetic grids towards isolating geophysically anomalous regions (anomalies). Vectorisation of potential field grids not only enables isolation and subsequent statistical analysis of anomalous areas, but also permits the use of geoprocessing tools to analyse spatial patterns. The methodology described in this report has been applied to the northern Gawler Craton, shown in Figure 1, which includes part of the Olympic Copper-Gold Province (Skirrow et al., 2007). Gravity and magnetic survey data covering the study area were reprocessed after the completion of the WPA Gravity Survey in 2013, providing gravity and TMI datasets with greater detail than previously available.

Zonal statistics extracted from the gridded datasets and embedded into the anomaly vectors (as attributes) include area, magnitude, minimum, maximum and average. The GIS polygons produced by the process can be used as mappable criteria for site selection and exploration targeting, since they represent regions of locally anomalous density or magnetic susceptibility. Anomaly contours constructed during the process provide additional detail of the property distribution within anomalous regions.

A data package accompanying this report contains a set of polygons for residual gravity and residual TMI attributed with descriptive statistics for the regions underlying each polygon; contours that indicate the distribution of potential field values within each polygon; polygon datasets with spatial clustering attribution and the residual potential field grids that were used to generate the vector datasets.

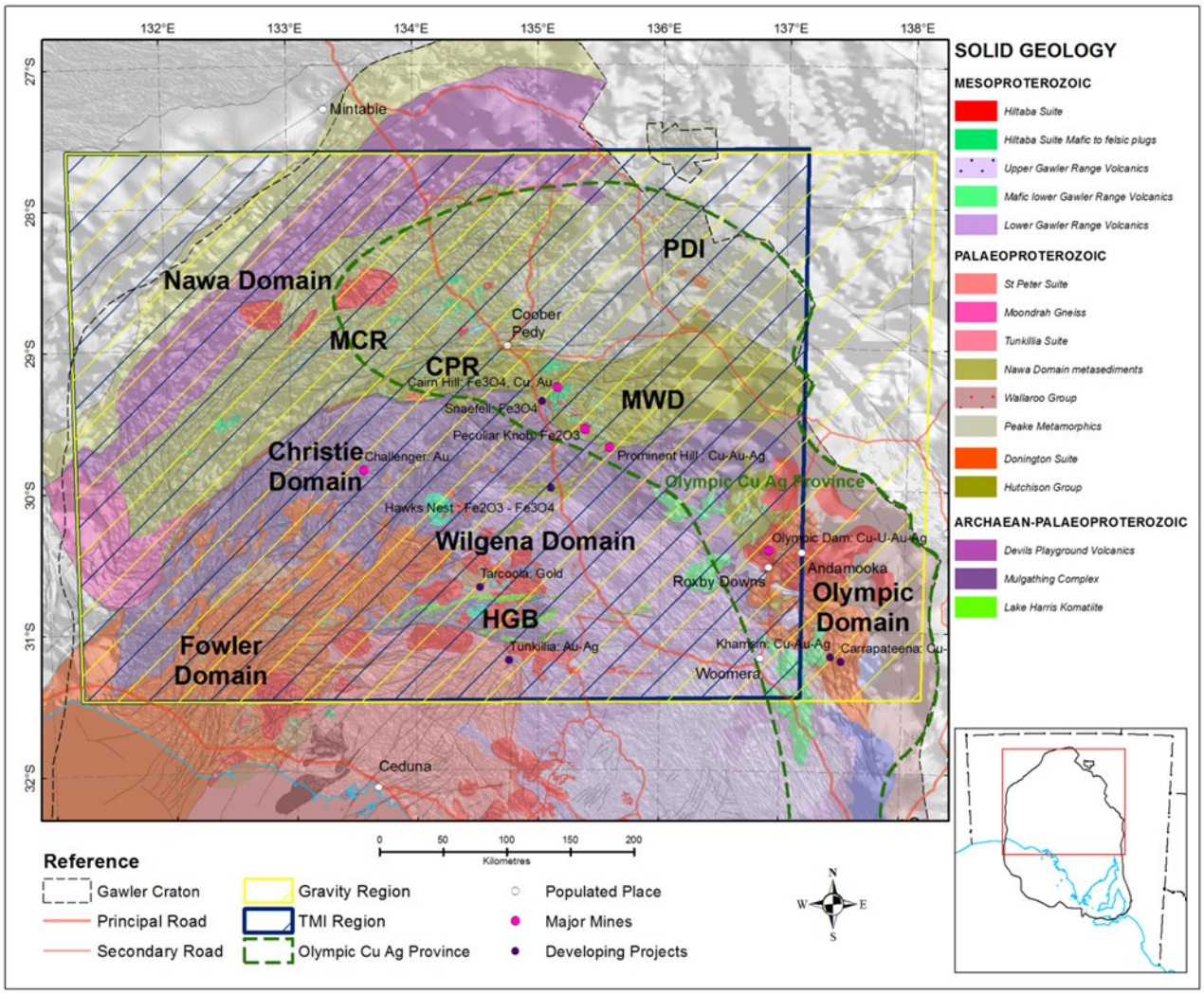

Figure 1. Location of the study area showing the extent of reprocessed gravity and magnetic data overlaying Archean-Mesoproterozoic solid geology of the Northern Gawler Craton, shaded by total magnetic intensity sunshade image. Geophysical domains and summary geology of the central-northern Gawler Craton are also shown. Abbreviations: MCR = Mabel Creek Ridge, CPR = Coober Pedy Ridge, MWD = Mount Woods Domain, PDI = Peake and Denison Inliers, HGB = Harris Greenstone Belt. (Plan number 205084-001)

GEOLOGICAL SETTING

The geology of the Gawler Craton is covered in detail in a number of papers including Daly, Fanning and Fairclough (1998); Ferris, Schwarz and Heithersay (2002); Hand, Reid and Jagodzinski (2007); Reid and Hand (2012). The Gawler Craton is composed of a Mesoarchean component, exposed on the north-eastern Eyre Peninsula along with two Neoarchean to early Paleoproterozoic belts, the southern Sleaford Complex and northern Mulgathing Complex that define the basement to the Proterozoic geology of the region. These belts were overlain and intruded by Paleoproterozoic sediments and magmatic rocks over the interval c. 2000 Ma through to c. 1730 Ma, before a major metamorphic and deformation event, the c. 1730–1690 Ma Kimban Orogeny occurred across the craton. Subsequent to this a number of magmatic suites were emplaced, particularly the St Peter Suite in the south-western portion of the craton, until a major magmatic event that produced felsic and mafic magmas of the Gawler Range Volcanics and Hiltaba Suite occurred in the early Mesoproterozoic, c. 1595–1570 Ma. This event was associated with widespread mineralisation (Skirrow, Bastrakov and Davidson et al., 2002; Drown, 2003; Ferris and Schwarz, 2003; Budd and Skirrow, 2007; Skirrow, Bastrakov and Barovich et al., 2007) and distributed deformation, the latter of which was termed the Kararan Orogeny (Daly, Fanning and Fairclough, 1998).

The Gawler Craton has been subdivided into a number of geophysically distinct domains, including the Coober Pedy Ridge (Fig. 1; Ferris, Schwarz and Heithersay, 2002). To the south the Christie and Wilgena domains, which are composed primarily of the Mulgathing Complex overlain by Paleoproterozoic sediments and Mesoproterozoic Hiltaba Suite and Gawler Range Volcanics. To the east lies the Mount Woods Domain, composed of iron-rich Paleoproterozoic metasediments (Mount Woods Complex and Skylark Metasediments) and Hiltaba Suite-related intrusives (Chalmers, 2007). Further to the south-east, the Olympic Domain contains low-grade Paleoproterozoic metasediments (Wallaroo Group) overlaying the Palaeoproterozoic Donington Suite, and are intruded and overlain by Hiltaba Suite and Gawler Range Volcanics (Fig. 1). To the north of the Coober Pedy Ridge lies the Mabel Creek Ridge and the Nawa Domain, composed principally of Paleoproterozoic metasediments, but with a number of rock units and metamorphic events that have no time equivalent in the southern Gawler Craton; c. 1920 Ma granite, c. 1515 Ma metamorphism and c. 1450 Ma magmatism and metamorphism (Jagodzinski and Reid, 2010; Howard, 2011). These younger events may have exerted a significant influence on the geology of the northern Gawler Craton and have certainly been responsible for exhumation and deformation along major shear zones in the region (Fraser and Lyons, 2006; Forbes, Giles and Jourdan et al., 2012; Fraser, Reid and Stern, 2012).

Cover thickness is highly variable across the wider northern Gawler Craton. Outcropping Archean to Mesoproterozoic is found best exposed in parts of the Wilgena Domain, such as around Tarcoola. Sparse outcrop is also observed in the Harris Greenstone Belt, the Fowler, Christie and Mount Woods Domains, and the Peake and Denison Inliers (Fig. 1). Thick Neoproterozoic-Cambrian cover sediments overlie the Gawler Craton to the east (Adelaide Geosyncline) and north/west (Officer Basin).

METHOD

A regional-residual separation was performed on Bouguer gravity and total magnetic intensity grids for the purpose of attenuating the response of sources which are assumed to originate at depths greater than the depth of investigation. Residual grids are commonly used for exploration targeting because they intensify what are believed to be near-surface or subtle features, resulting in an image with higher contrast (Langenheim et al., 2011) and greater detail.

The regional residual separation method used to produce the residual grids for both magnetics and gravity was the subtraction of an upward continued grid from the original grid (Langenheim and Hildenbrand, 1997). The residual grid was then processed to produce GIS polygons (vectorisation) delineating anomalous regions, which were tagged with the zonal statistics of the underlying grid regions. For the purpose of this discussion, an anomalous region is a localised area of higher potential field value than the area immediately surrounding it and is spatially defined as a region delineated by a closed contour, whose inner portion's potential field value is higher than the value of the contour defining the region's boundary.

INPUT GRIDS

The gravity and magnetic grids used for, and generated by this analysis are summarised in Table 1.

Table 1. Gravity and TMI grids, extents and cell size used in the analysis.

Grid name	**Grid extent** (lat and long of bounding coordinates)	**Cell size**
WPA Gravity	Top: -27.53, Right: 138.39, Bottom: -31.5, Left: 131.1	100 m
WPA Gravity Residual	Top: -27.53, Right: 138.39, Bottom: -31.5, Left: 131.1	100 m
WPA TMI	Top: -27.58, Right: 137.17, Bottom: -31.48, Left: 131.24	35 m
WPA TMI RTP	Top: -27.58, Right: 137.17, Bottom: -31.48, Left: 131.24	35 m
WPA TMI RTP Residual	Top: -27.53, Right: 138.39, Bottom: -31.5, Left: 131.1	35 m

GRID PREPARATION (GRAVITY)

1. The gravity grid was upward continued to 1000 m (Fig. 2).
2. The upward continued grid was subtracted from the original grid to produce a residual gravity grid (Fig. 3), using the following formula:

   $OutputGrid_{Residual} = InputGrid - InputGrid_{UC1000}$ ¬where
   InputGrid is the potential field grid (Bouguer gravity or RTP TMI)
   $InputGrid_{UC1000}$ is the InputGrid upward continued to 1000 metres

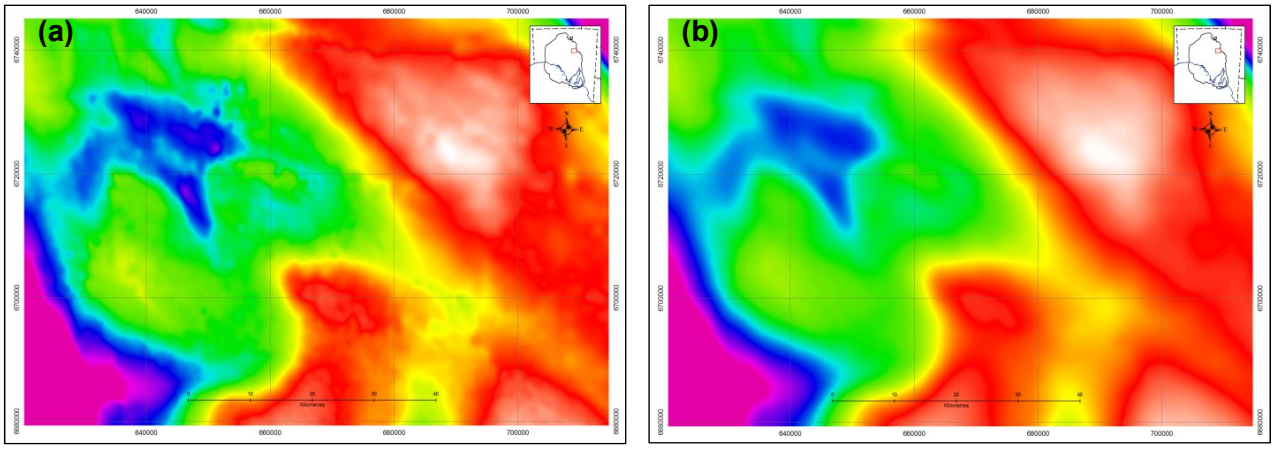

Figure 2. Subset region within the study area, displaying gravity (a) and gravity upward continued 1000 m (b). The upward continued gravity is a smoother image with less detail, representative of the response from deep sources.

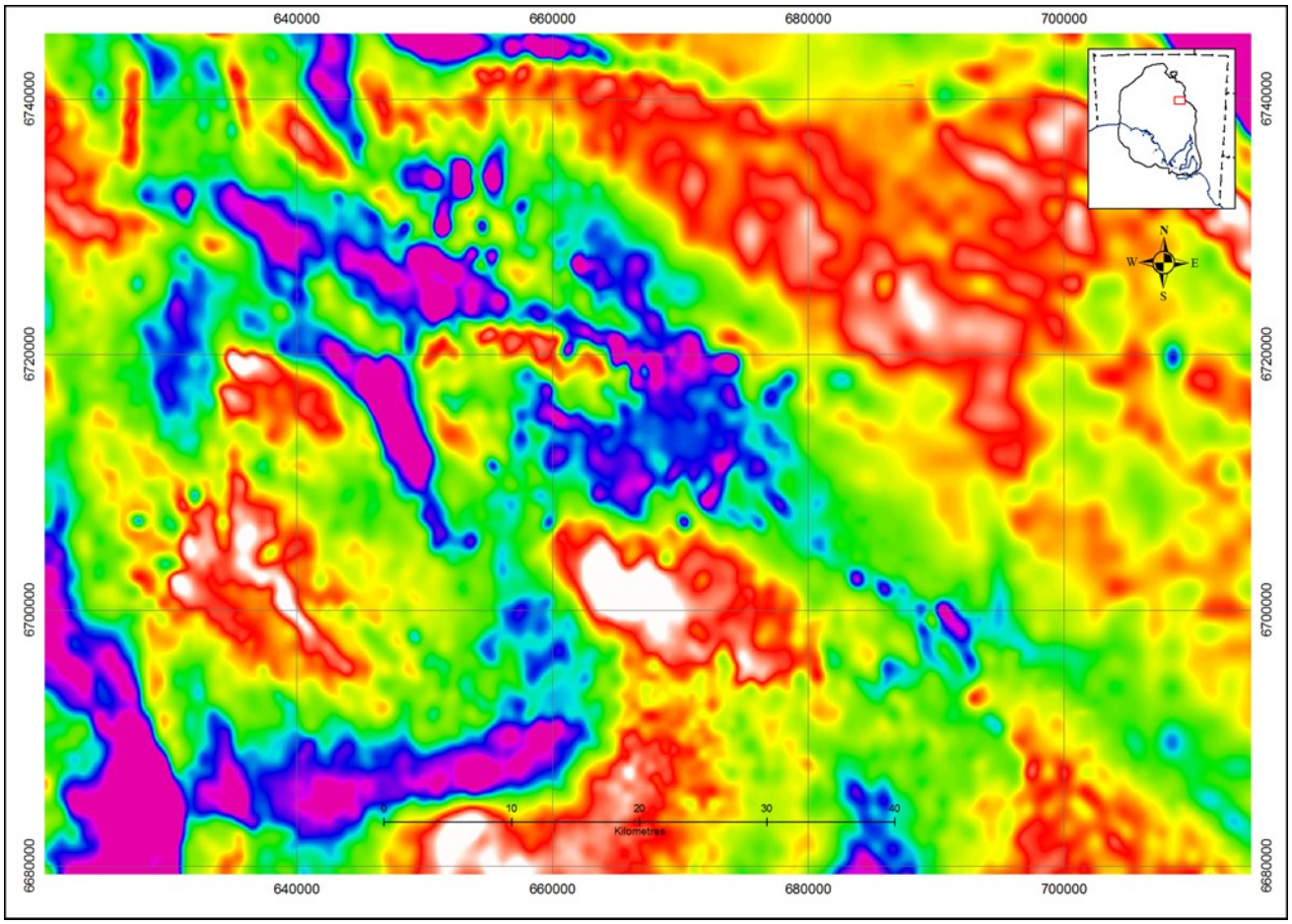

Figure 3. The same subset region within the study as that shown in Figure 2, displaying residual gravity (Gravity – Gravity upward continued 1000 m). The residual grid attenuates deeper sources and intensifies features thought to be nearer the surface.

GRID PREPARATION (TMI)

1. A reduction to pole was performed on the TMI grid, using a single value in the centre of the magnetic grid and the year 2000 for the IGRF calculation (Fig. 4a).
2. The resulting magnetic grid was upward continued to 1000 m (Fig. 4b).
3. The upward continued grid was subtracted from the original grid to produce a residual RTP TMI grid (Fig. 5), using the formula shown in step 2, Grid preparation (Gravity).

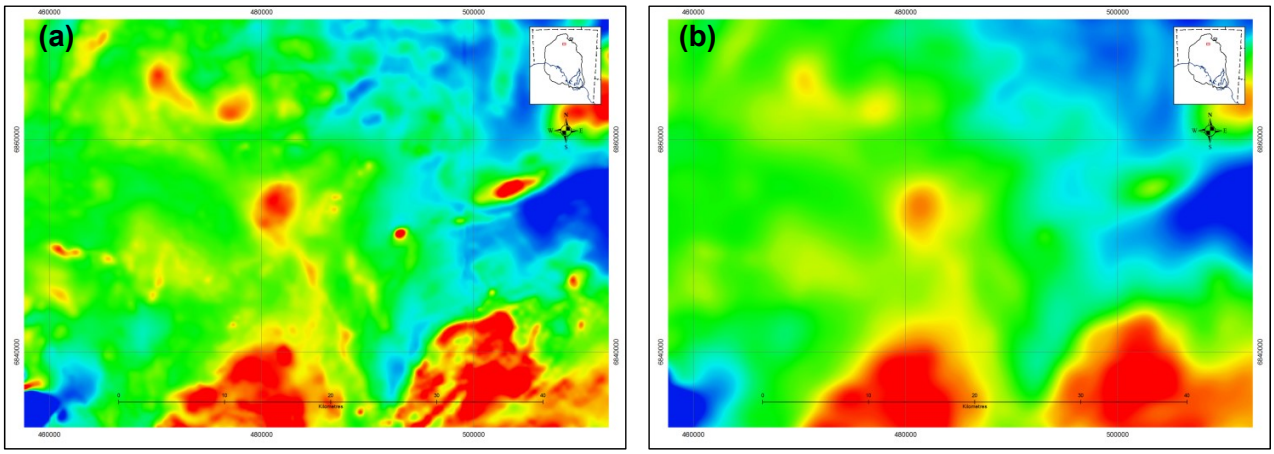

Figure 4. Subset region within the study area, displaying reduced to pole TMI (a) and Reduced to pole TMI upward continued 1000 m (b).

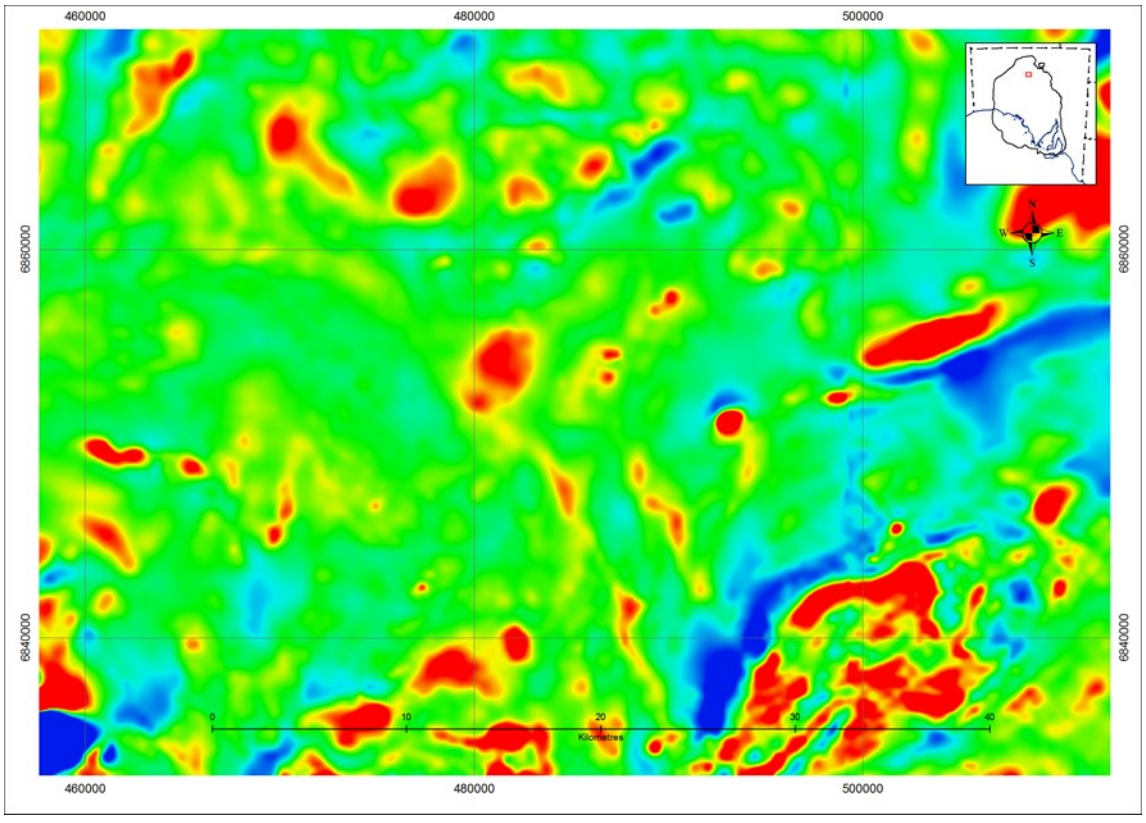

Figure 5. The same subset region within the study as that shown in Figure 4, displaying residual TMI (Reduced to pole TMI – Reduced to pole TMI upward continued 1000 m).

DELINEATION OF GEOPHYSICAL HIGHS FROM EACH GRID, USING A GEOPROCESSING SCRIPT (ARCGIS), APPLIED TO $OUTPUTGRID_{RESIDUAL}$

The following nine steps were performed within the ArcGIS Model Builder environment to vectorise (convert gridded data into vector data) geophysical anomalies within the residual grids.

1. Contours were generated at an interval defined by the analyst as a script parameter. Optimally, a very small contour interval should be used to produce the densest possible set of contours, within the memory limitations of the computer used for the processing. 0.1 milliGal (mGal) was used for gravity and 5 nanoTesla (nT) was used for TMI (Fig. 6).
2. A perimeter distance threshold was determined by the analyst as a script parameter. The perimeter distance is used by the routine to select closed contours that are less than or equal to the distance threshold. After a number of tests using various different distance thresholds, the distances used for this study were 30 km for gravity datasets and 60 km for magnetic datasets. These thresholds delineated discrete anomalies. Thresholds that were too small tended to delineate regions within the central portion of an anomalous region, while thresholds that are too large delineate multiple anomalies within an anomalous region.
3. The contours generated during step 2 were converted to polygons and dissolved (generating a single feature from each set of contours representing an anomaly), before being attributed with the contour value at the perimeter of each anomalous region.
4. Centroids (the geographic central point) of these polygons were generated and the grid value underlying each centroid was transferred to the centroid as an attribute.
5. The centroid value was transferred to its parent polygon using a spatial join. Each polygon therefore contains two attributes: a centroid value and a perimeter (contour) value.
6. Potential field anomalies were defined within the script by selecting polygons whose centroid value exceeded the perimeter value (Fig. 7). Polygons whose centroid value was lower than the perimeter value were discarded.
7. The anomaly polygons were intersected with the residual grid and “zonal statistics” were calculated as additional polygon attributes. The additional attributes captured from the residual grid include the mean of raster cell values within an anomaly (MN), minimum raster cell value within an anomaly (MIN), maximum raster cell value within an anomaly (MAX), standard deviation of raster cell values within an anomaly (STD), sum of raster cell values within an anomaly (SUM), count of raster cells within an anomaly (CNT), and range of values within an anomaly (RNG), equivalent to MAX-MIN.
   The polygon-grid intersect operation uses the following rule: a polygon must intersect the centroid of a cell in order for the cell to be included in the computation. The cell count (RES_CNT) therefore indicates the number of cell centroids intersecting the polygon feature. The overlay concept used to compute the statistics is illustrated in Figure 8.
8. A “magnitude” was calculated by subtracting the perimeter contour value from the MAX attribute. Table 2 displays the attribute table of a subset of the TMI polygon dataset.
9. It was noted that in the TMI dataset, a small number of 60 km perimeter anomalies enveloped multiple smaller, discreet anomalies. In these cases, the 60 km anomaly polygons were manually deleted and replaced with 30 km anomalies, generated as a separate run of the script.

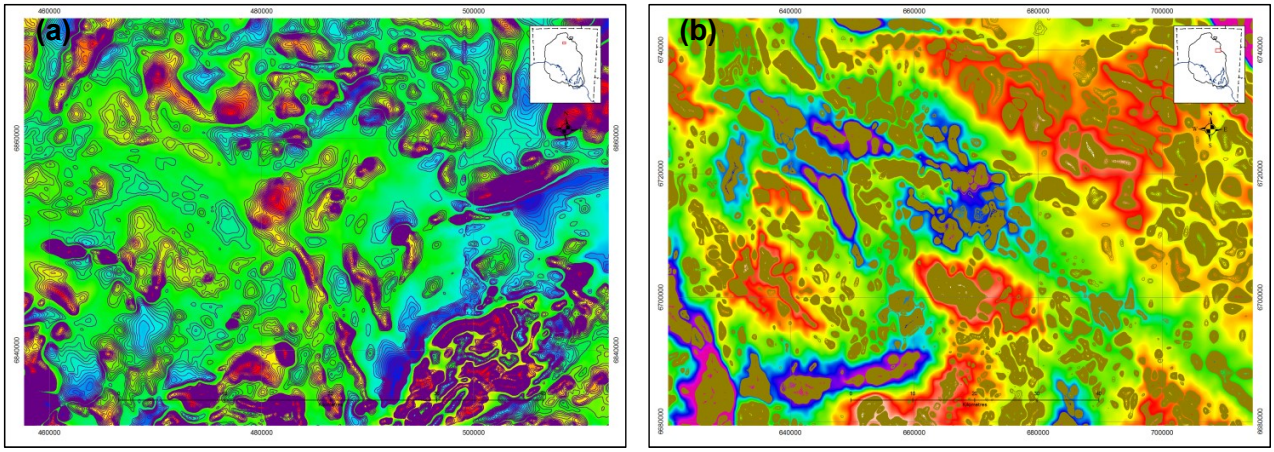

Figure 6. TMI contours up to 60 km in length (a) and gravity contours up to 30 km in length (b). Note: the density of the gravity contours (0.1 mGal contour interval) makes them appear as solid objects.

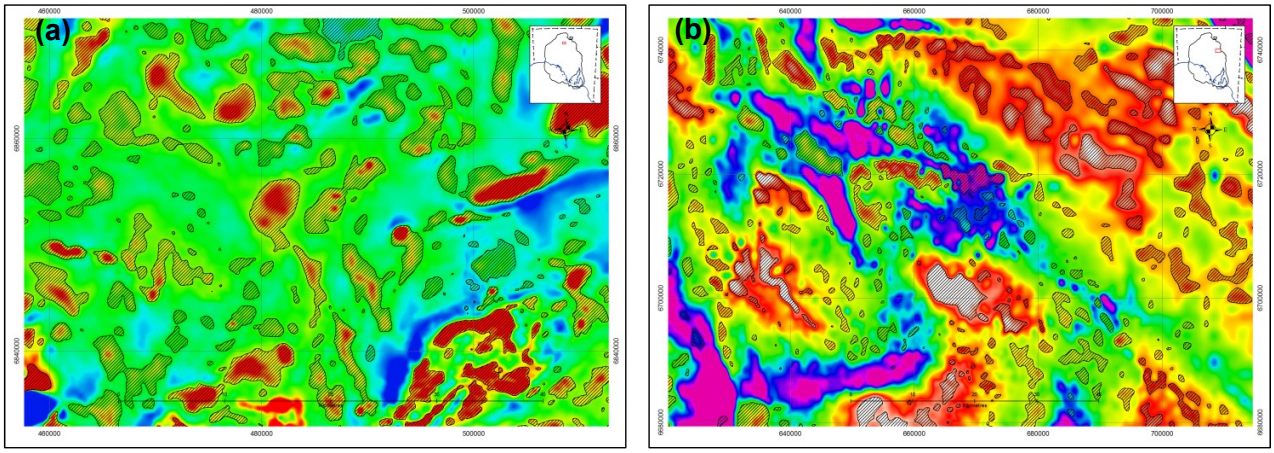

Figure 7. Anomalies outlined by polygons whose centroid value exceeds the perimeter value; TMI (a) and gravity (b).

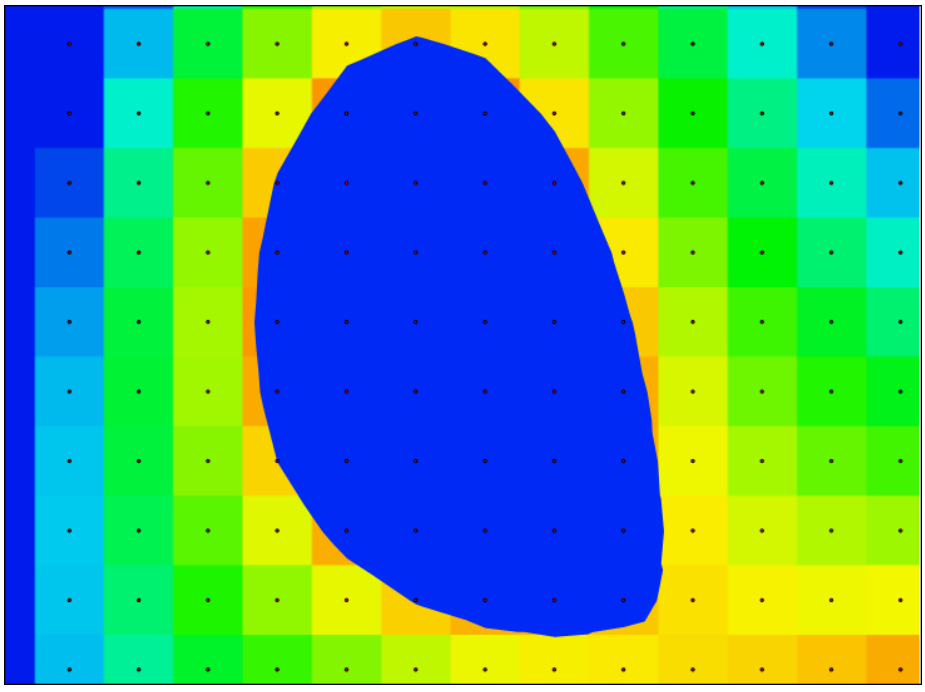

Figure 8. Centroids of grid cells are shown intersecting an anomaly polygon. The grid cells of intersected centroids are used in the statistical calculations for each feature. RES_CNT for this feature is 41.

Table 2. **Excerpt from the attribute table for magnetic anomalies polygon dataset displaying zonal statistics: minimum (RES_MIN), maximum (RES_MAX), mean (RES_MN), standard deviation (RES_STD), count of cells within each polygon (RES_CNT), sum of cells within each polygon (RES_SUM), range (RES_RNG), and Magnitude (calculated by subtracting Contour from MAX).**

Contour	RES_MIN	RES_MN	RES_MAX	RES_STD	RES_CNT	RES_SUM	RES_RNG	Magnitude	Shape_Len	Shape_Area
0	0.17	42.92	116.4	30.34	224	9614	116.23	116.4	4809	321948
0	0	5.31	15.81	5.44	15	48	15.81	15.81	486	11894
-75	-74.85	-74.82	-74.79	0.03	2	-150	0.06	0.21	163	463
40	43.74	43.74	43.74	0	1	44	0	3.74	76	270
95	95.03	119.54	159.09	14.95	282	33711	64.06	64.09	3099	331599
5	6.34	41.49	86.28	24.14	24	996	79.95	81.28	813	33076
0	5.83	7.92	10.69	2.04	3	24	4.86	10.69	319	5945
-5	-5	1.05	8.1	4.21	20	21	13.1	13.1	598	22947
285	286.26	327.73	387.23	28.99	93	30479	100.97	102.23	1397	107649
-75	-74.69	-68.52	-61.83	3.98	39	-2672	12.86	13.17	890	48601
0	0.35	84.83	177.64	54.05	235	19934	177.29	177.64	2113	295726
20	20.01	59.34	128.17	27.5	1232	73105	108.16	108.17	8427	1524994
0	0.09	4.67	9.36	2.63	62	290	9.27	9.36	1496	76543
70	70.06	210.56	526.91	110.39	1481	311843	456.85	456.91	7057	1827204
-65	-64.87	5.72	190.69	65.65	498	2848	255.56	255.69	3352	608264
35	35.08	41.11	48.66	3.91	90	3700	13.58	13.66	1228	111581
-65	-63.99	-63.27	-62.03	0.79	5	-316	1.95	2.97	273	4958
0	0.26	27.42	80.15	17.18	288	7897	79.89	80.15	3073	367184
90	90.17	92.78	94.92	2.02	7	649	4.75	4.92	305	6746
0	0.19	4.31	8.63	2.88	10	43	8.45	8.63	375	10679
70	70.1	82.34	95.83	7.77	98	8069	25.73	25.83	1252	116330
-45	-44.88	-29.82	-8.49	9.8	325	-9692	36.39	36.51	2709	394569
-100	-99.91	-82.68	-56.24	12.53	234	-19348	43.67	43.76	2000	288089
0	0	111.42	312.79	72.14	1193	131815	312.79	312.79	6687	1479142
70	70.09	134.53	224.29	45.9	465	62555	154.2	154.29	2844	569389
-25	-24.79	-1.09	46.8	16.35	405	-441	71.6	71.8	4239	497215
-95	-94.52	-82.25	-68.11	7.79	72	-5922	26.41	26.89	1141	88979

DATASET CHECKS AND MANUAL CLEAN-UP

This methodology succeeded in delineating more than 99% of residual anomalies within the geophysical grids. Some anomalies were erroneously omitted by the routine because they have a central low area within the anomalous region (found in TMI datasets). In these cases the script incorrectly identified the region as a "low" because the centroid was placed within the inner low region, making the centroid value lower than the perimeter value. An example of this is shown in Figure 9 and was manually corrected by selecting the relevant anomaly from the original contour data and appending it to the anomaly polygon dataset. The datasets were checked for other such anomalies and they were corrected. A further visual check was performed to identify the polygons mentioned in step 9 that delineate multiple anomalies as a single region, due to the 60 km distance threshold. These polygons were deleted and replaced with polygons encapsulating individual anomalies generated by running the script with a 30 km distance threshold.

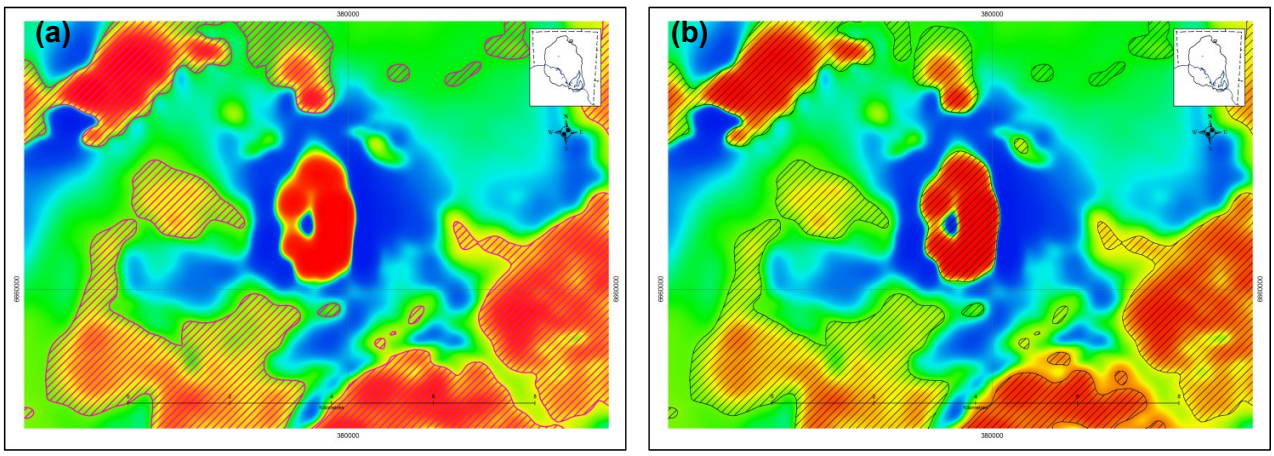

Figure 9. **TMI dataset checking and correction.** **(a)** illustrates the issue of an anomaly not selected by the automated routine due to central low in the TMI feature at the centre of the figure; **(b)** anomaly subsequently delineated and appended by selecting and

polygonising the appropriate contour from the contour dataset generated by the geoprocessing routine.

Edge effects in the gravity image caused by gridding artefacts near the perimeter of the grid were identified visually and spurious polygons tagged. Tagging was performed by creating a numeric field named “Exclude” in the dataset attribute table and populating the attribute with the number 1, in order to differentiate between features to exclude and features to keep. This provides a mechanism for optionally filtering out unwanted features without permanent deletion. Small polygons of less than 50,000 m^2 in area were also tagged to exclude. 50,000 m^2 equates to 5 pixels for gravity and 40 pixels for TMI, due to the differing cell sizes of each grid. Due to their small size, these anomalies can be ignored for most regional analyses and interpretation. The “shape area” field, created automatically by ArcGIS allows further filtering by anomaly area.

The final step of dataset preparation was to spatially join the anomaly polygon attributes to the contour datasets generated by the process, to enable the contour datasets to be filtered by the same parameters as the anomaly polygons. This adds utility to the contour data and also has advantages when using both the anomaly polygons and the contour data together, because it allows the same filter to be applied to both the polygon and contour datasets.

DATA CLASSIFICATION AND CLUSTER MAPPING

The magnitude attribute in the polygon datasets was calculated by subtracting the contour value at the edge of each anomaly from the maximum value within each anomaly. When the anomaly dataset is classified on the magnitude attribute, high magnitude anomalies appear to spatially cluster. This can be seen in Figures 10 and 16. To determine that the observed clustering is statistically non-random, a high-low clustering analysis was performed on the gravity and TMI anomaly datasets using the High/Low Clustering Getis-Ord General G statistic which identifies the degree of clustering of high or low values (de Smith et al., 2015). Clustering was determined to be non-random with high magnitude anomalies displaying clustering in both the magnetics and gravity datasets. The High/Low clustering (Getis-Ord General G) tool is a spatial statistics tool in the ArcGIS software package.

Satisfied that high magnitude clustering is non-random, a cluster and outlier analysis was performed on the magnitude attribute of the gravity and TMI anomaly datasets using a Cluster and Outlier Analysis (Anselin Local Moran’s I; Anselin, 1995), which identifies and maps clusters of high and low magnitude anomalies as well as high and low magnitude outliers (ESRI, 2013). The Cluster and Outlier Analysis (Anselin Local Moran’s I) is a spatial statistics tool in the ArcGIS software package.

RESULTS

GRAVITY DATA

Gravity grids, TMI grids and grid statistics are presented in Appendix 1. The gravity anomaly polygons are displayed in Figure 10 using a natural breaks classification, which bases classes on natural groupings within the data (de Smith et al., 2015).

To determine the effect of gravity station density on anomaly generation, a density of gravity station grid was produced. This is displayed in Figure 11 and shows that in areas where there is a higher density of gravity stations a higher number of gravity anomalies were delineated. The outline of the Northern Olympic Domain survey (2007) and the Woomera Prohibited Area survey (2013) can be seen in the data and was expected due to the higher detail inherent in a grid produced by the higher density of gravity station spacing within those surveys. Conversely, the regions with sparse gravity station spacing produced correspondingly sparse, rounded anomaly geometries.

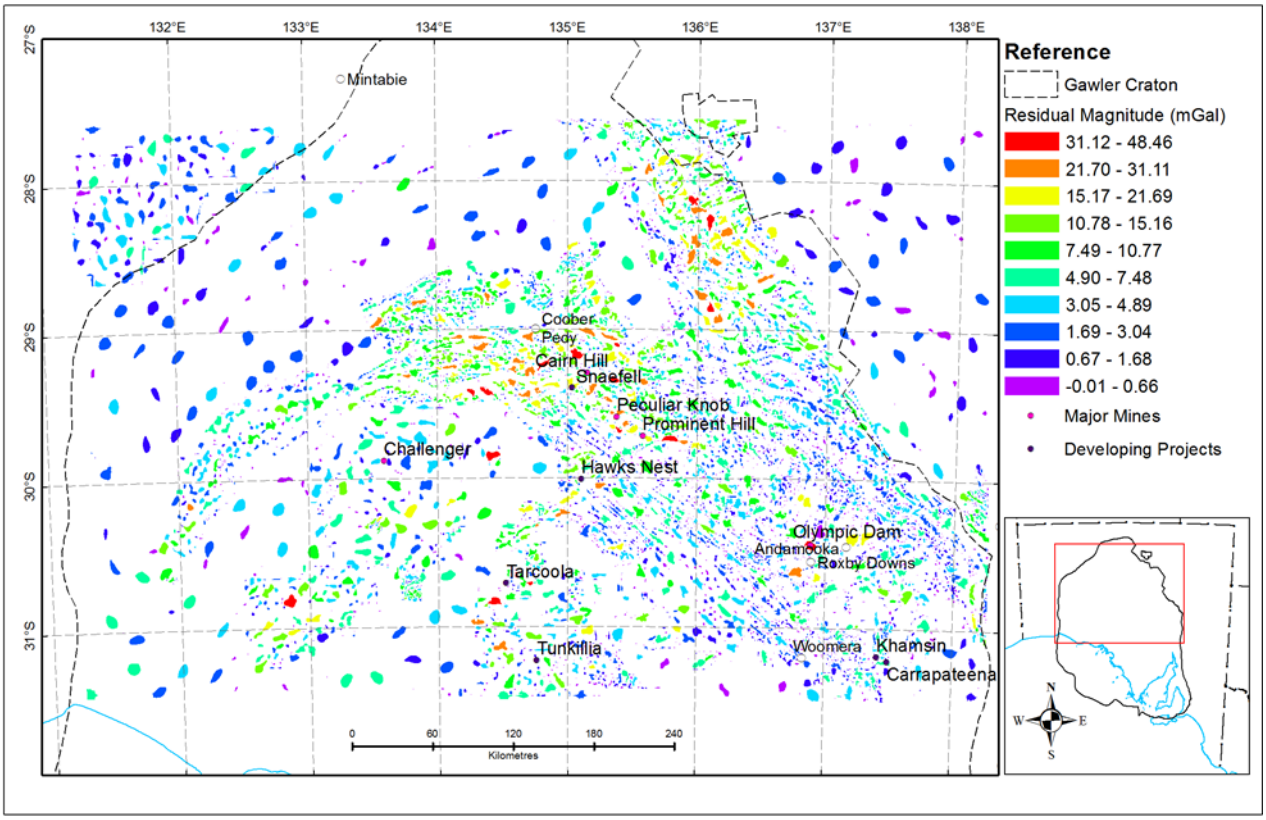

Figure 10. Residual gravity anomaly polygons symbolised by anomaly magnitude (MAX – Contour). Warmer colours indicate high magnitude anomalies. High magnitude anomalies appear to spatially cluster. (Plan number 205084-002)

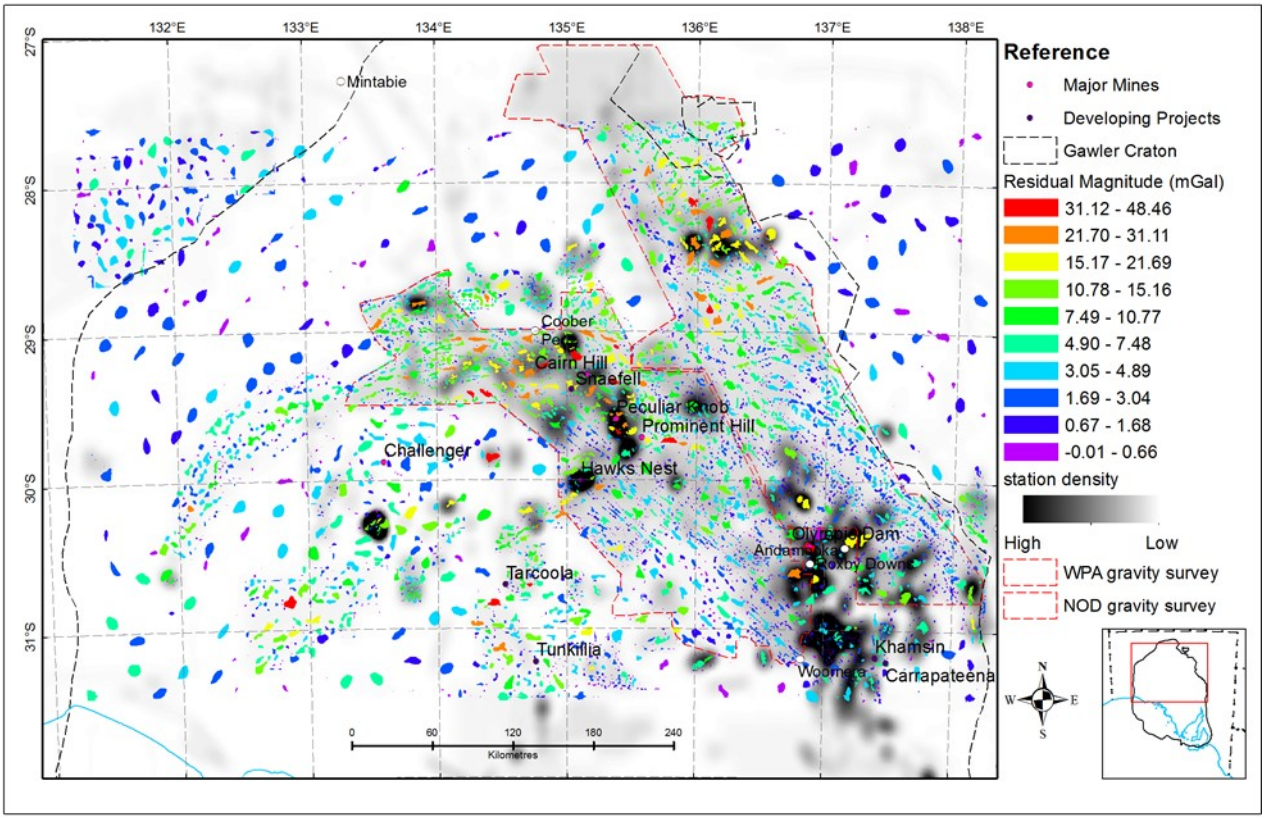

Figure 11. A gravity station density grid broadly corresponds with a higher number of delineated anomalies per unit area.

Table 3 displays the highest and lowest values of the residual gravity dataset attributes.

The range of values for residual magnitude of gravity anomaly is -0.01 to 48.46 mGal. The anomaly with the highest residual magnitude is located at the Wilgena Hill iron ore deposit, shown in Figure 12. The range for residual maximum anomaly value is -53.2 to 97.8 mGal. The anomaly with the highest maximum is located adjacent to the Peculiar Knob iron ore mine, shown in Figure 13. Peculiar Knob also has the highest mean value of 77.7 mGal.

Table 3. High and low values of polygon attributes for residual gravity.

Residual Gravity (mGal, rounded to one decimal point)		
Attribute	*Polygon, highest value*	*Polygon, lowest value*
Magnitude	48.5	0.0
Range	48.4	0.0
Mean	77.7	-53.5
Min	69.0	-53.7
Max	97.8	-53.2
Std Dev	13.6	0.0

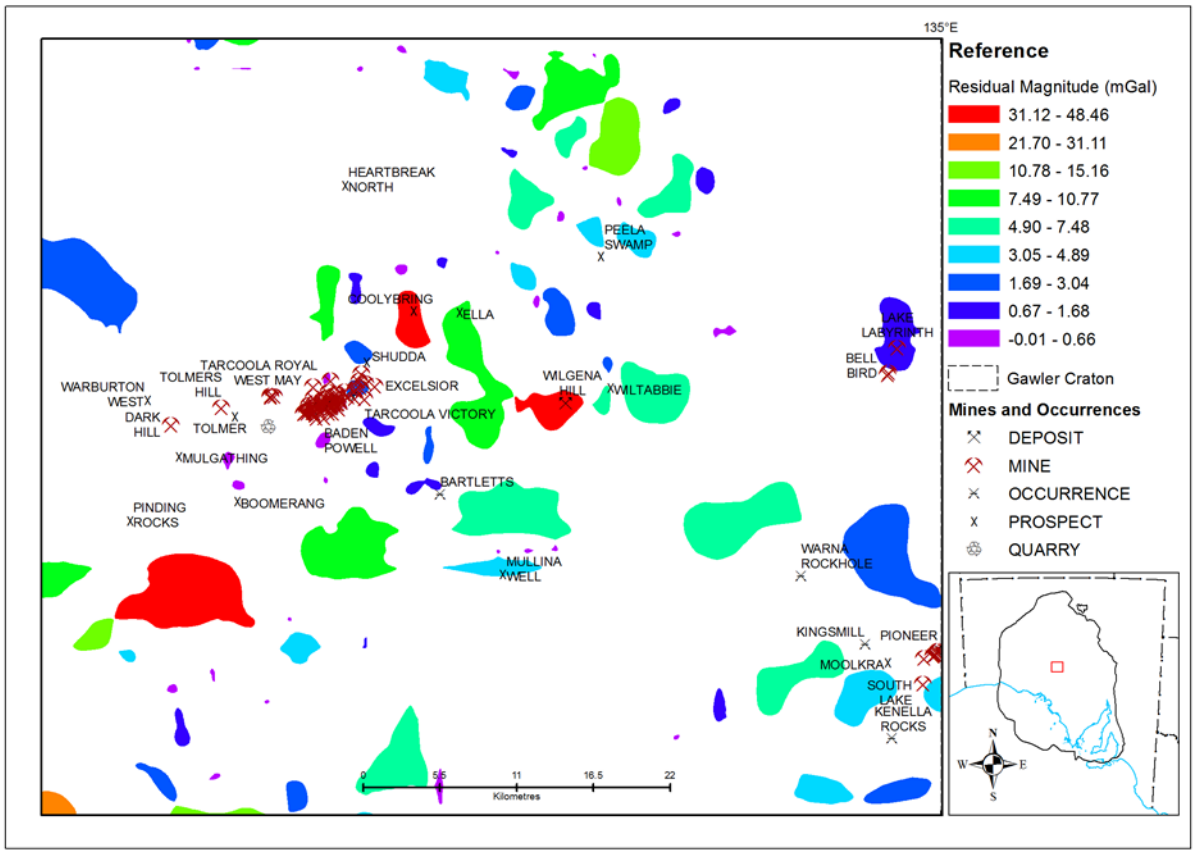

Figure 12. The Wilgena Hill iron ore deposit has the highest anomaly magnitude recorded by the anomaly processing routine at 48.5 mGals.

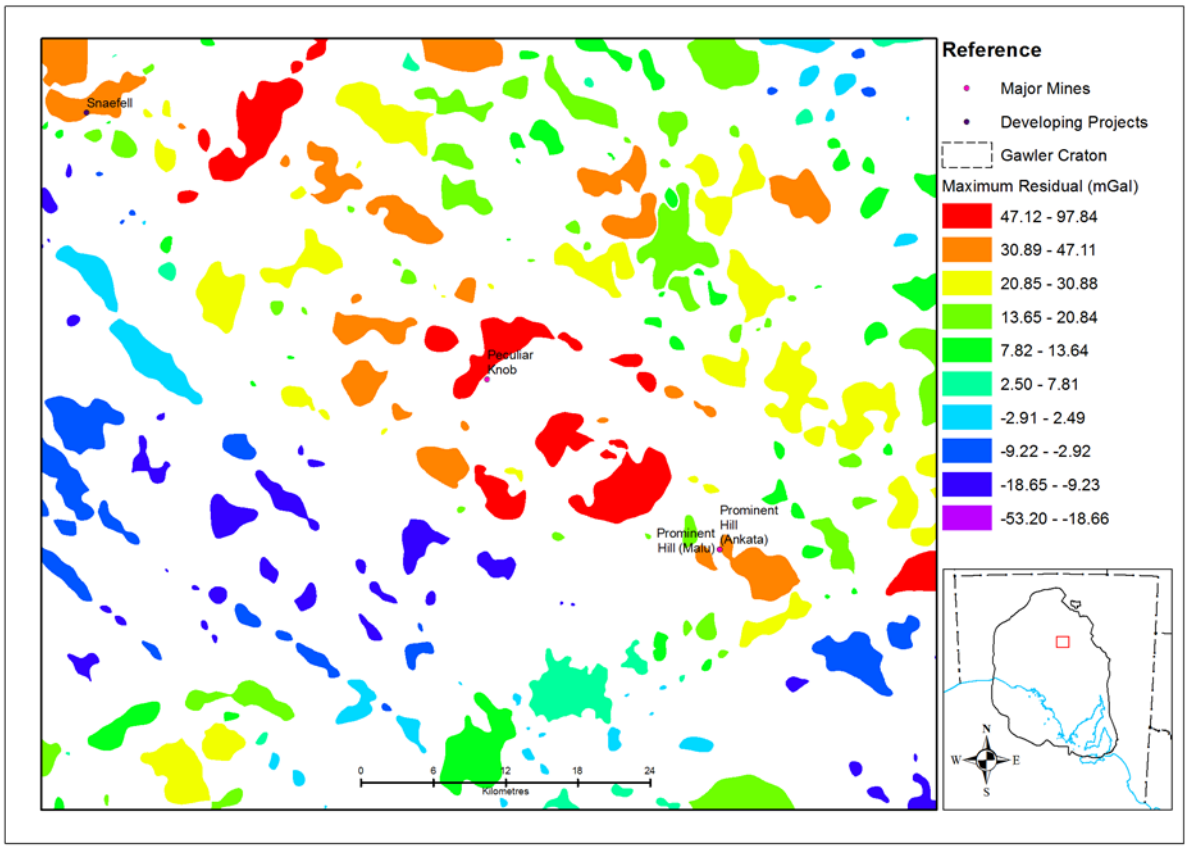

Figure 13. The Peculiar Knob iron ore mine has the highest anomaly maximum recorded by the anomaly processing routine at 97.8 mGals and the highest mean value at 77.7 mGals.

The high-low clustering analysis was performed on the gravity anomaly dataset using the Getis-Ord General G statistic to determine if high or low magnitude anomalies are spatially associated (Getis and Ord, 1992). The high-low clustering report is produced by the High/Low clustering (Getis-Ord General G) tool in ArcGIS and is displayed in Figure 14. The null hypothesis states that there is no spatial clustering of high magnitude gravity anomalies. The result of the clustering analysis using the Getis-Ord General G statistic reveals a z-score of 13.099757, indicating that the null hypothesis can be rejected and clustering of high magnitude gravity anomalies is not random. Clusters of high magnitude gravity anomalism are associated with underlying geology or geological processes. The extent of clustering may coincide with the extent of petrophysical domains that can also be explained geologically.

With clustering of high magnitude gravity anomalies determined, the ArcGIS cluster and outlier analysis (Anselin Local Moran's I; Anselin, 1995) tool was applied to the magnitude attribute of the gravity anomaly dataset. The analysis identifies statistically significant hot spots, cold spots and spatial outliers by calculating a local Moran's I, a z-score and p-value and determines whether the null hypotheses of no local spatial association is accepted or rejected on a feature by feature basis (ESRI, 2013; Anselin, 1995). The output indicates whether the apparent similarity of either high or low values or dis-similarity (a spatial outlier) is more pronounced than what would be expected in a random distribution. The results are presented as four cluster/outlier types: HH for a statistically significant (0.05 level) cluster of high values; LL for a statistically significant (0.05 level) cluster of low values; HL for a feature with a high value surrounded by low values and LH for a low value surrounded by high values. The analysis used a search radius of 37.139 km, which is the Euclidean distance that ensures every feature has at least one neighbour and is the neighbourhood used in the analysis for each anomaly. The cluster and outlier map is displayed in Figure 15 and shows low clustering and high-low clustering almost exclusively in the south eastern region, broadly coincident with the Olympic Domain. Several outliers occur at the rim of the Peake and Denison Inliers and in the Western part of the Christie Domain. Broad areas of high clustering are observed in the Coober Pedy Ridge, Mabel Creek Ridge, Mount Woods Domain, Peake and Denison Inliers. Further high clusters exist in the Fowler, Christie and Wilgena Domains.

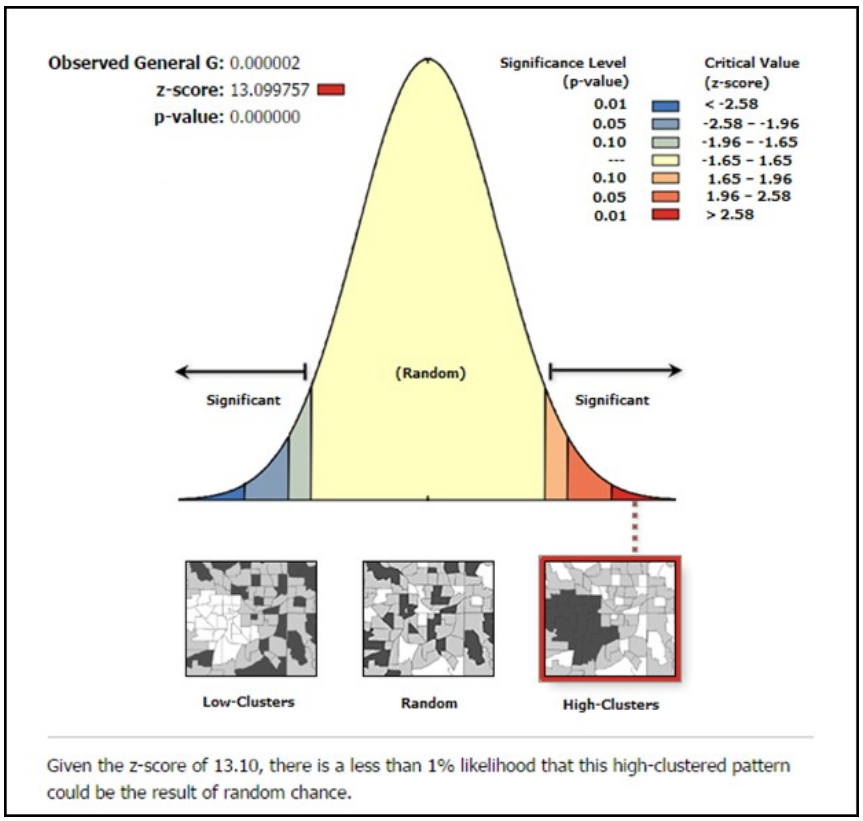

Figure 14. The figure is generated by the ArcGIS High/Low clustering (Getis-Ord General G) tool and demonstrates the output of the Getis-Ord General G analysis. The z-score of 13.099757 indicates high magnitude gravity anomaly clustering across the study area is non-random.

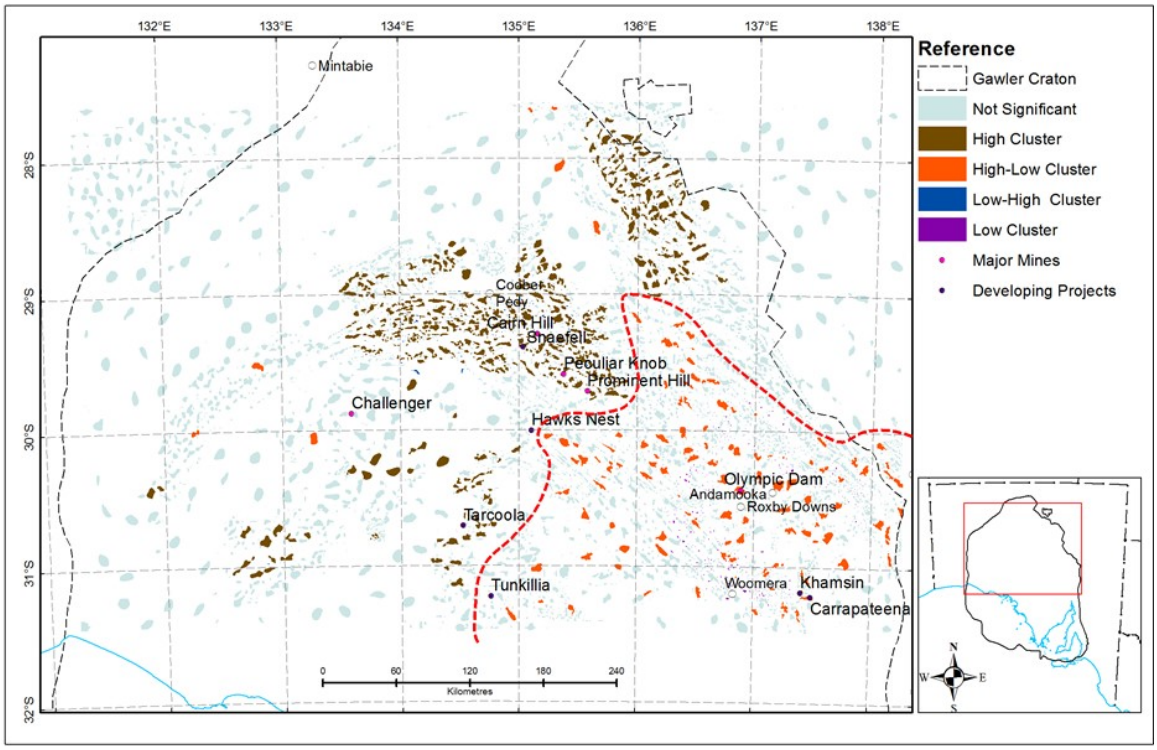

Figure 15. The cluster outlier analysis of gravity anomaly magnitude reveals clustering of high magnitude anomalies over the Coober Pedy Ridge, Mabel Creek Ridge, Mount Woods Domain and Peake and Denison Inliers. High-low clusters (outlier anomalies) are evident in the Eastern Gawler Province. The red line delineates the extent of a region of high-low clusters covering the Olympic Domain. (Plan number 205084-003)

TMI DATA

Table 4 displays the highest and lowest values of the residual TMI attributes.

Table 4. High and low values of polygon attributes for residual TMI.

Residual TMI (nT, rounded to whole numbers)		
Attribute	*Highest value*	*Lowest value*
Magnitude	18521	0
Range	19043	0
Mean	7152	-756
Min	4093	-1785
Max	18416	-735
Std Dev	3984	0

The TMI anomaly polygons are displayed in Figure 16, using a natural breaks classification.

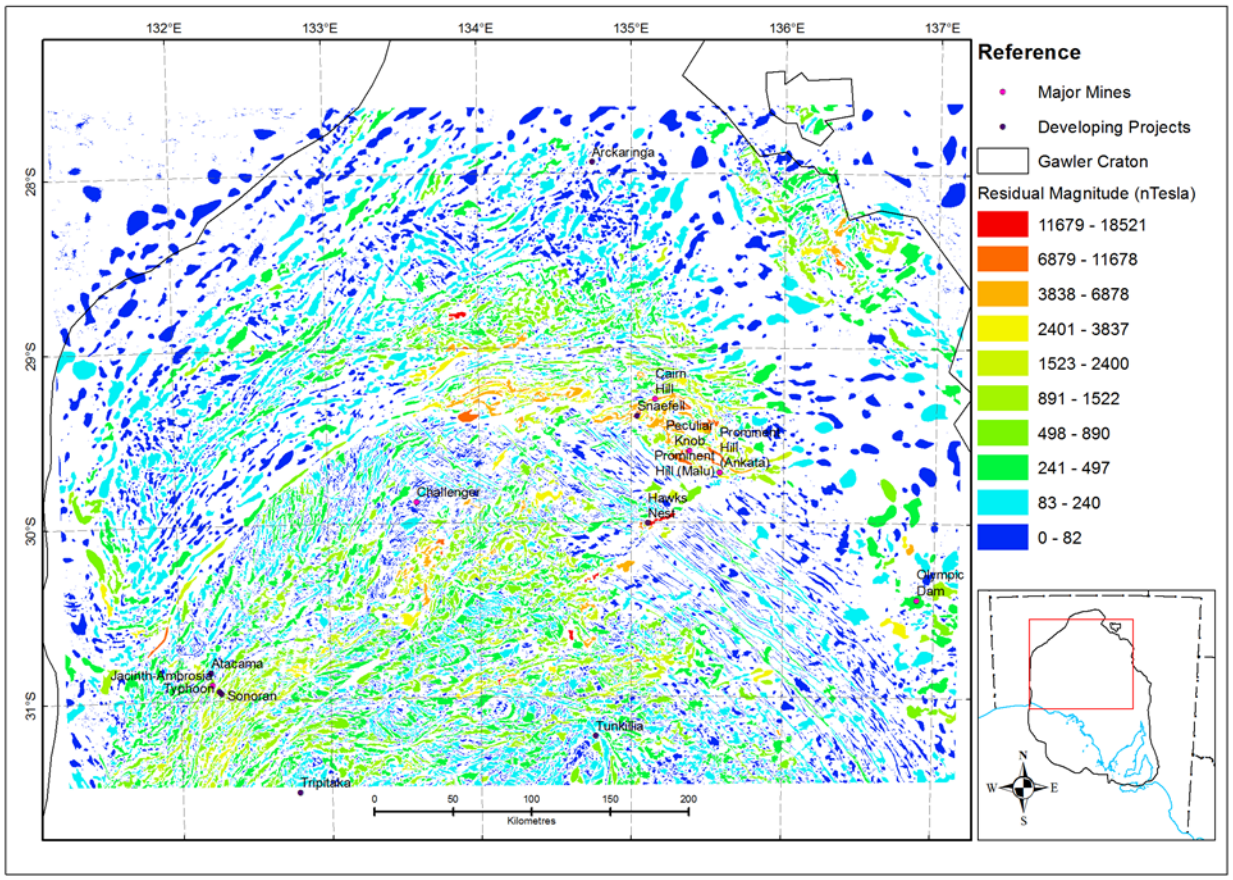

Figure 16. Residual RTP TMI anomaly polygons symbolised by anomaly magnitude (MAX – Contour). Warmer colours are indicative of high magnitude anomalies. (Plan number 205084-004)

The range of values for residual magnitude of TMI anomaly is 0–18521 nT. High range magnetic intensity is often related with magnetite (Fe_3O_4) and associated iron oxide deposits. The anomaly with the highest residual magnitude and highest maximum (18416 nT) is located at the Giffen Well iron deposit, shown in Figure 17.

Spatial statistics were performed on the magnetic anomalies to determine if high magnitude anomalies are randomly distributed throughout the region or are spatially correlated. The null hypothesis states that there is no spatial clustering of high magnitude magnetic anomalies. The result of a clustering analysis using the Getis-Ord General G statistic (Fig. 18) reveals a z-score of 5.288189 indicating that the null hypothesis can be rejected and that clustering of high magnitude magnetic anomalies is not random. Figure 19 shows the high-low clustering report.

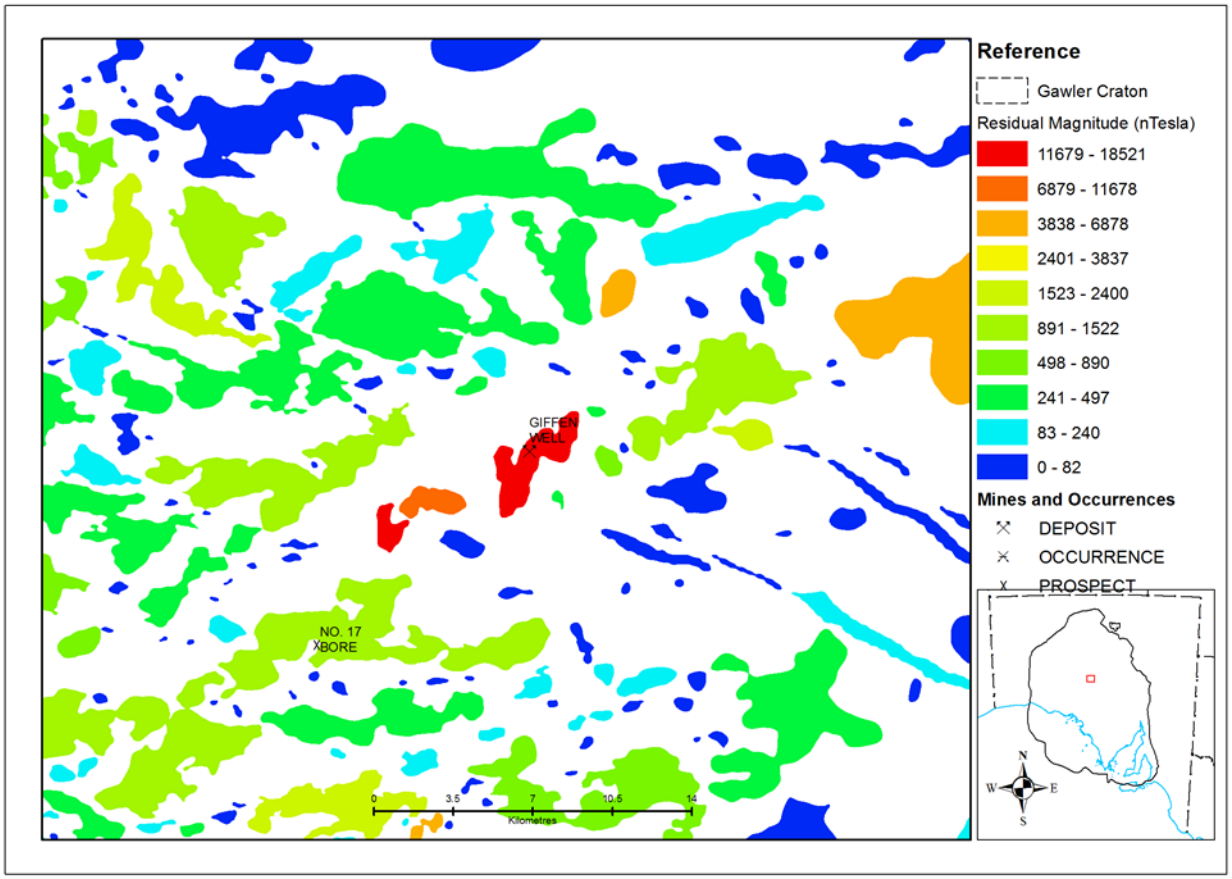

Figure 17. The Giffen Well deposit has the highest anomaly magnitude and maximum recorded by the anomaly processing routine at 18520 nT.

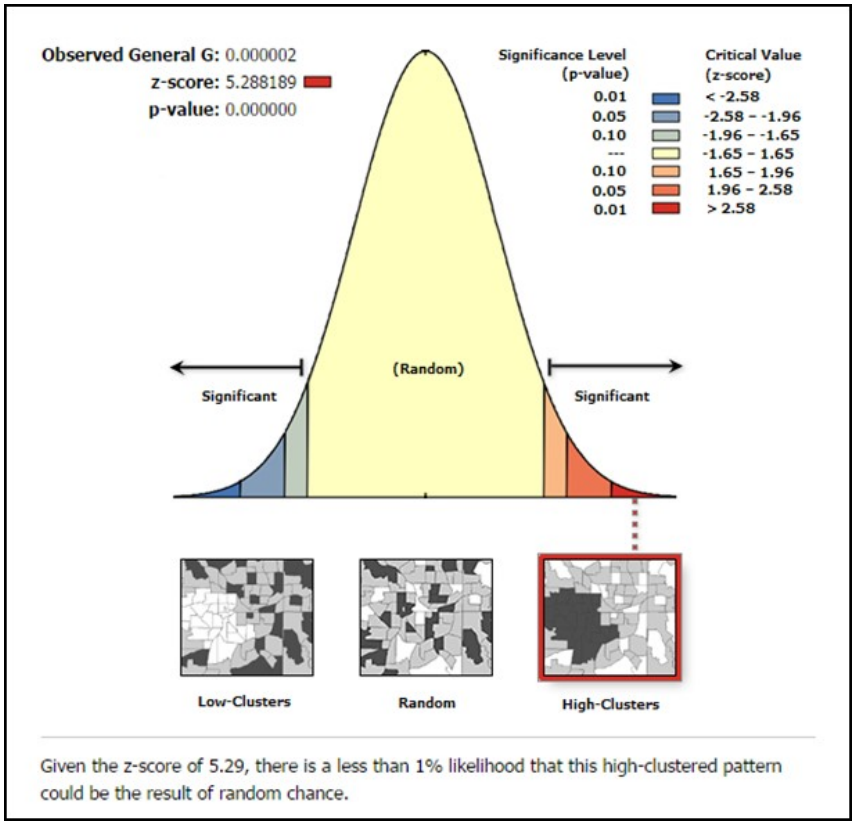

Figure 18. The Getis-Ord General G statistic is used to determine if apparent clustering of high or low magnitude magnetic anomalies is the result of random chance. The z-score of 5.29 indicates significant, non-random high clusters. The figure is generated by the ArcGIS High/Low clustering tool.

With clustering of high magnitude magnetic anomalies determined, the Anselin Local Moran's I cluster and outlier analysis was run in ArcGIS on the magnitude attribute of the TMI anomaly dataset. The clusters and outliers are displayed in Figure 19. Clustering of high magnitude TMI anomalies is concentrated over the Mabel Creek Ridge, Coober Pedy Ridge, Mount Woods Domain, Peake and Denison Inliers, Christie Domain, Wilgena Domain, Fowler Domain and the Harris Greenstone Belt. High-low clusters are fewer in number and occur between the High clusters. A few high clusters and high-low outliers were found in the Olympic Domain.

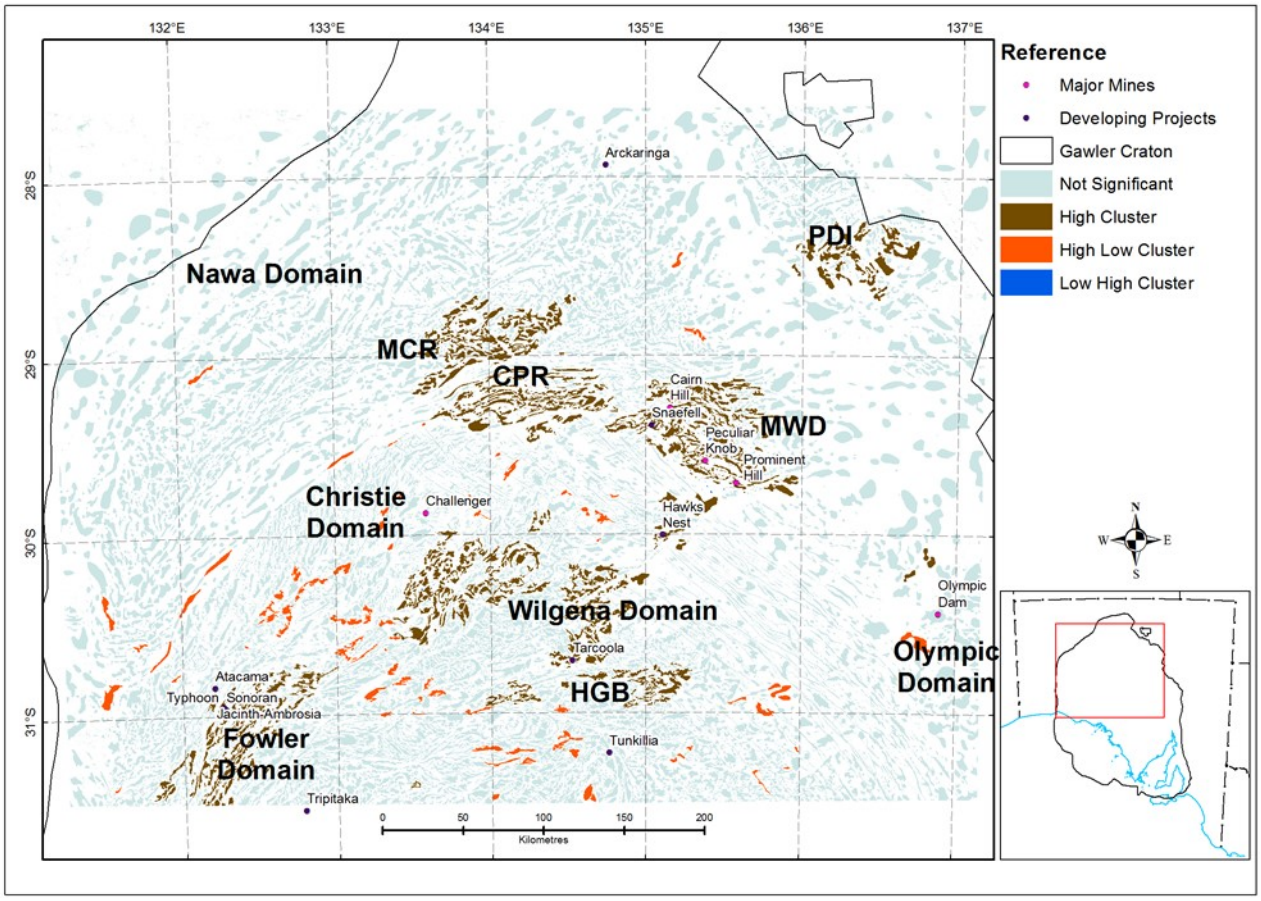

Figure 19. The cluster analysis of TMI anomaly magnitude reveals clustering of high magnitude anomalies over Coober Pedy Ridge, Mabel Creek Ridge, Mount Woods Domain, Peake and Denison Inliers, Wilgena Domain, Fowler Domain and the Harris Greenstone Belt. High-low clusters occur mainly across the southern half of the study area. Abbreviations: MCR = Mabel Creek Ridge, CPR = Coober Pedy Ridge, MWD = Mount Woods Domain, PDI = Peake and Denison Inliers, HGB = Harris Greenstone Belt. (Plan number 205084-005)

CONTOUR DATASETS

The polygon attributes were spatially joined to the contour datasets that were generated as part of the geoprocessing routine. The contours were then used for interpretation, utilising the same filters as applied to the polygons. The contours show a more detailed property distribution within an anomaly, as illustrated in Figure 20.

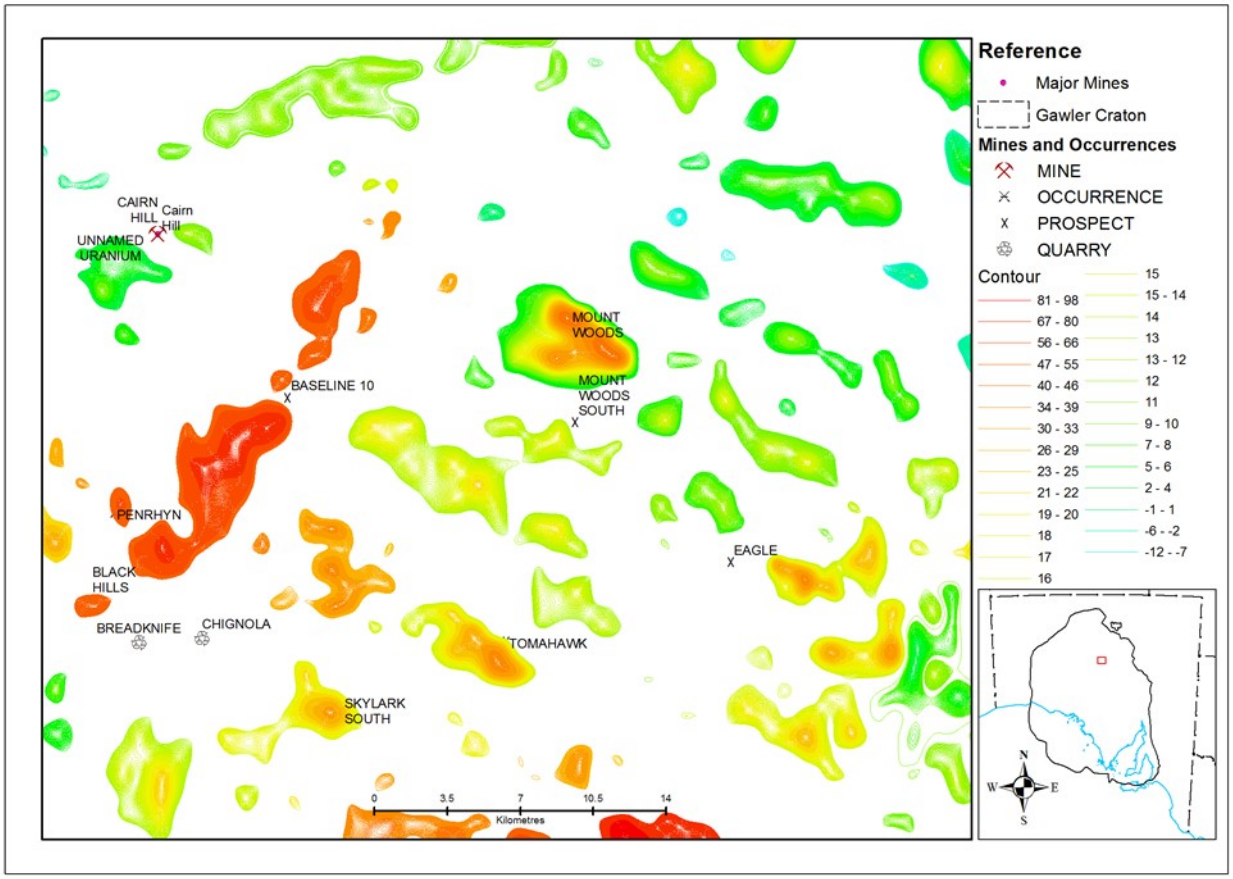

Figure 20. Contours within gravity anomalies provide an indication of the distribution of residual gravity within anomalous regions.

COINCIDENT ANOMALIES

Coincident anomalies are regarded as gravity and magnetic anomalies that are spatially overlapping or within close proximity of one another. A GIS process can make selections based on spatial location of both gravity and magnetic anomalies that are within a given distance from each other. This enables further filtering to be performed when exploring for commodities that are characterised by coincident potential field anomalies. Figure 21 illustrates coincident anomalies for the study area using a distance of up to 1000 m separation to infer coincidence. Figure 22 illustrates coincident anomalies using a distance of up to 100 m to infer coincidence. Anomalies with separation distances of 0–100 m and 0–1000 m have been captured as attributes in the polygon tables, enabling anomalies outside these distance thresholds to be filtered out. Further analysis can be carried out in GIS, using any or no distance threshold. A comparison of the 1000 m threshold with the 100 m threshold reveals significant differences in the number of polygons filtered. There were 4259 gravity polygons within 1000 m of a TMI polygon and 3524 within 100 m of a TMI polygon. There were 8856 TMI polygons within 1000 m of a gravity polygon and 5705 within 100 m of a gravity polygon. This illustrates the concept of reducing the search space using filters within the GIS environment.

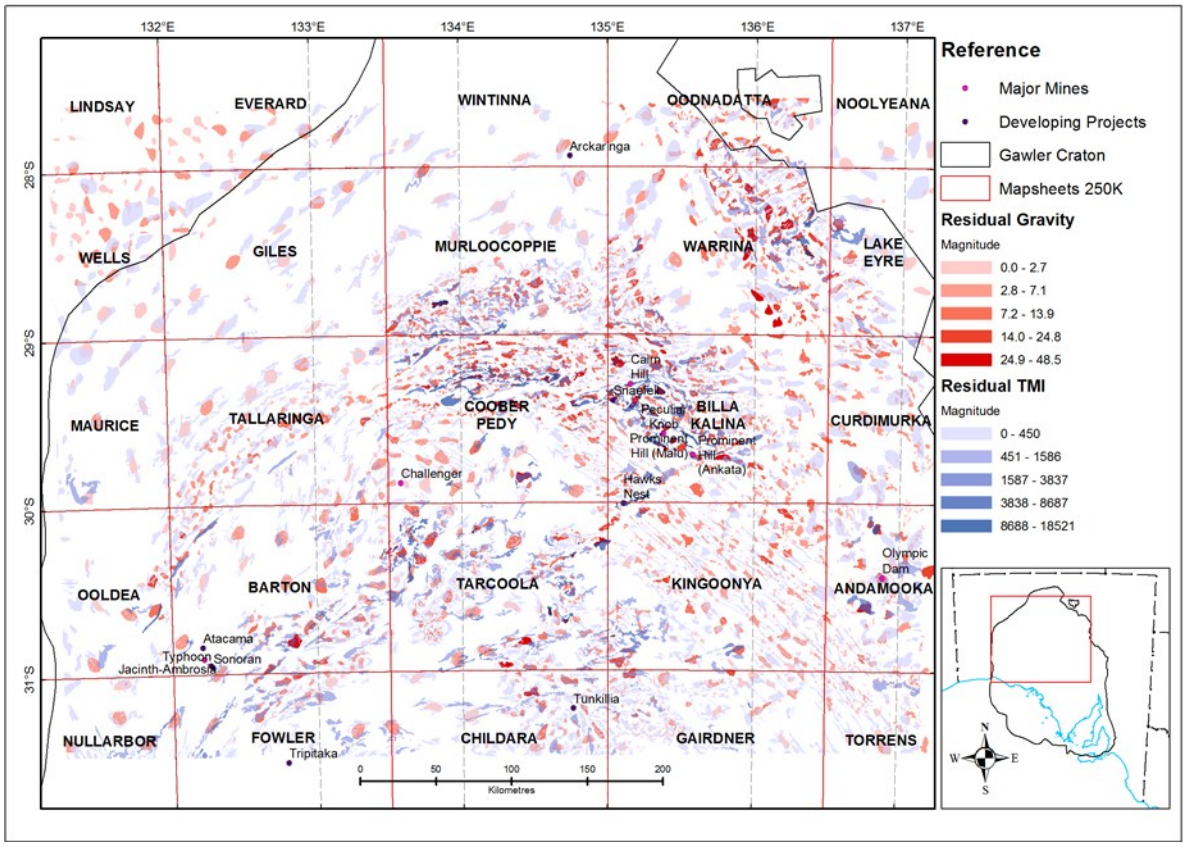

Figure 21. Spatially coincident gravity and TMI anomalies. In this example 1000 m lateral separation is considered coincident, resulting in 8856 TMI polygons and 4259 gravity polygons. (Plan number 205084-006)

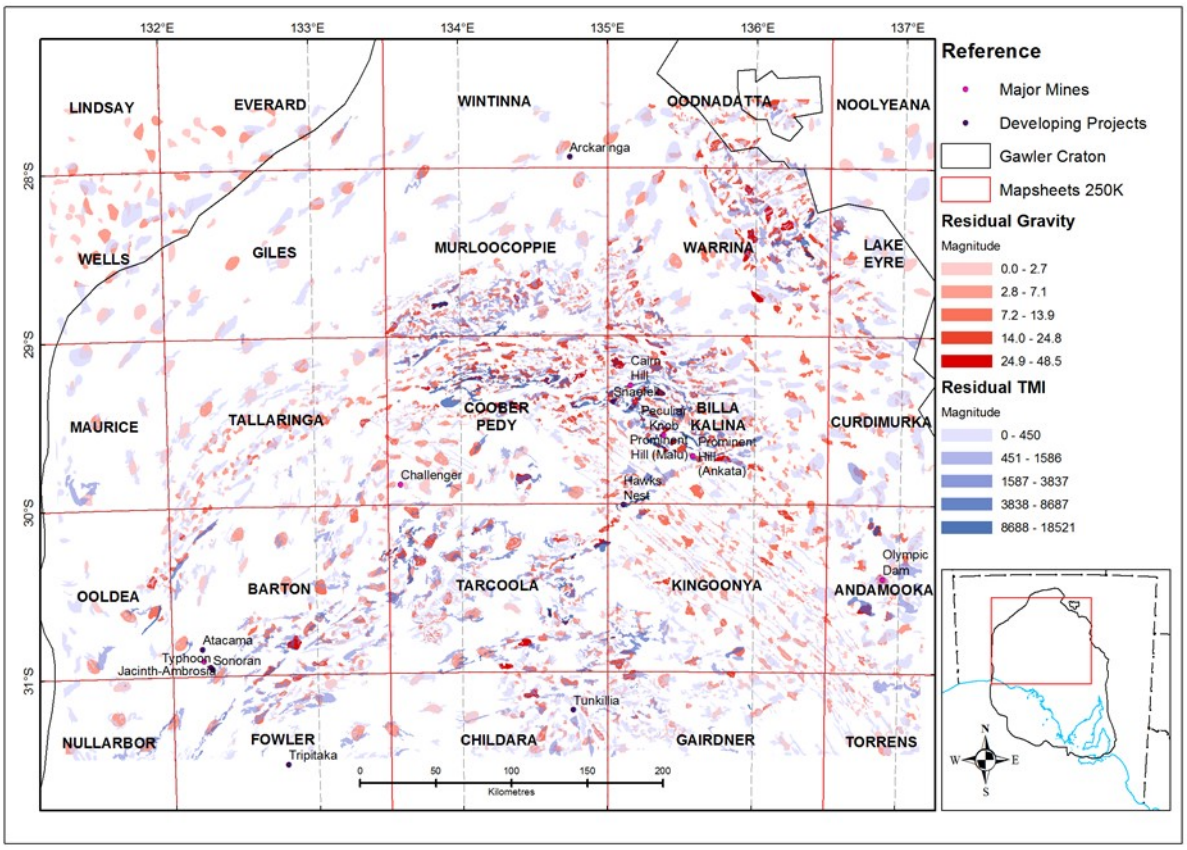

Figure 22. Spatially coincident gravity and TMI anomalies. In this example 100 m lateral separation is considered coincident resulting in 5705 TMI polygons and 3524 gravity polygons. (Plan number 205084-007)

DISCUSSION

RATIONALE

The geoprocessing techniques that extract potential field anomalies from gridded datasets and joins attributes to those anomalies was designed to produce datasets that can be used for regional site selection, quantitative analysis and mineral potential modelling applications. Early trials of the technique (in which anomalies were generated but not attributed) were successful in delineating a large proportion of the known IOCG deposits and prospects in the Eastern Gawler Province at that time, including the subsequently discovered Khamsin deposit, but also delineated subtle anomalies that were highlighted by the residual techniques. The filtering capabilities provided by the addition of polygons attributes make it possible to filter, threshold and thereby control how anomalies are selected for a given analysis, based on anomaly magnitude, anomaly size or spatial correlation with other anomalies. This provides the capability to rank anomalies by their magnitude or other attribute, or fit attribute ranges to known deposits for direct comparison between those deposits and anomalies of similar value.

TECHNIQUE TO GENERATE A RESIDUAL FIELD

Various techniques for producing a regional residual separation of potential field data (most commonly gravity) have been used for decades (Gupta and Ramani, 1980; Hearst and Morris, 2001; Zeng et al., 2007; Langenheim et al., 2011). Many of the techniques elucidated in the literature have one thing in common: subtraction of a regional field from the original data to produce a residual field. The main difference among many of the techniques has been the approach used to derive or optimise the regional field for a given study region.

For this study, the choice of the upward continuation technique and 1000 m for the upward continuation distance for generating the regional field resulted from trials performed by the Geological Survey of South Australia in 2009 on a large portion of the Eastern Gawler Craton, using subsets of national datasets (produced by Geoscience Australia) at resolutions of 800 m for gravity and 200 m (resampled from 80 m) for total magnetic intensity. The resulting residual grids generated from 1000 m upward continued datasets delineated the gravity and magnetic signatures of most of the well-known IOCG deposits in the Olympic eastern Gawler Craton. Moreover, all of these IOCG deposits and occurrences displayed a gravity anomaly with a magnetic anomaly either in close lateral proximity (within 1000 m) or coincident.

ZONAL STATISTICS ATTRIBUTES

The zonal statistics attributes quantify the anomaly polygons, providing the basis for numerical and statistical analysis. The magnitude attribute is the main focus of this discussion because it provides a measure of an anomaly in relation to its immediate surroundings. Filters and classifications applied to the magnitude attribute appear to result in plausible representations of underlying geology and processes.

Magnitude is calculated by subtracting the anomaly contour value from the maximum value within the anomaly. Range (RES_RNG) is calculated by subtracting the minimum raster cell value within an anomaly from the maximum value. The key difference between magnitude and range is that the raster cell minimum is not always identical to the contour value, because some anomalies contain a low region within an otherwise high region, as illustrated in Figure 23. In that example, a reversely magnetised region can be seen within a broader magnetic high region. The contour value is 10 nT while the minimum value of the region is -302 nT. The maximum value is 138 nT, therefore the magnitude and range respectively are 128 nT and 440 nT. The magnitude attribute arguably provides a more effective measure of an anomaly for analysis and modelling (particularly magnetic anomalies) because it is not confounded by remanent magnetic features within an anomalous zone or limitations of the fixed perimeter distance parameter, which can outline a region that contains values both lower and higher than its defining contour. Remanent features causing a significant difference between magnitude and range are not common within the study area.

Both the ‘Magnitude’ and ‘Range’ attributes provide a sense of the rate of change of magnetic response within an anomaly region and provide an effective filtering mechanism. For example, subtle anomalies can be filtered out leaving only higher magnitude features. Figure 24 displays an example of a 1000 nT threshold applied to the magnitude value of the TMI dataset.

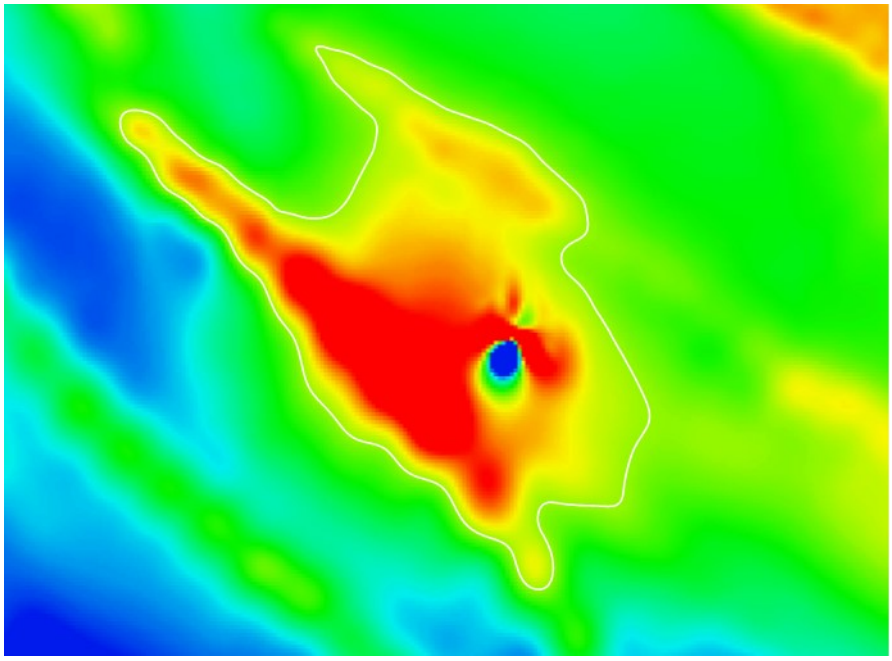

Figure 23. A reversely magnetised region within an anomaly produces a magnetic minimum that is lower than the value of the contour at the perimeter of the anomaly.

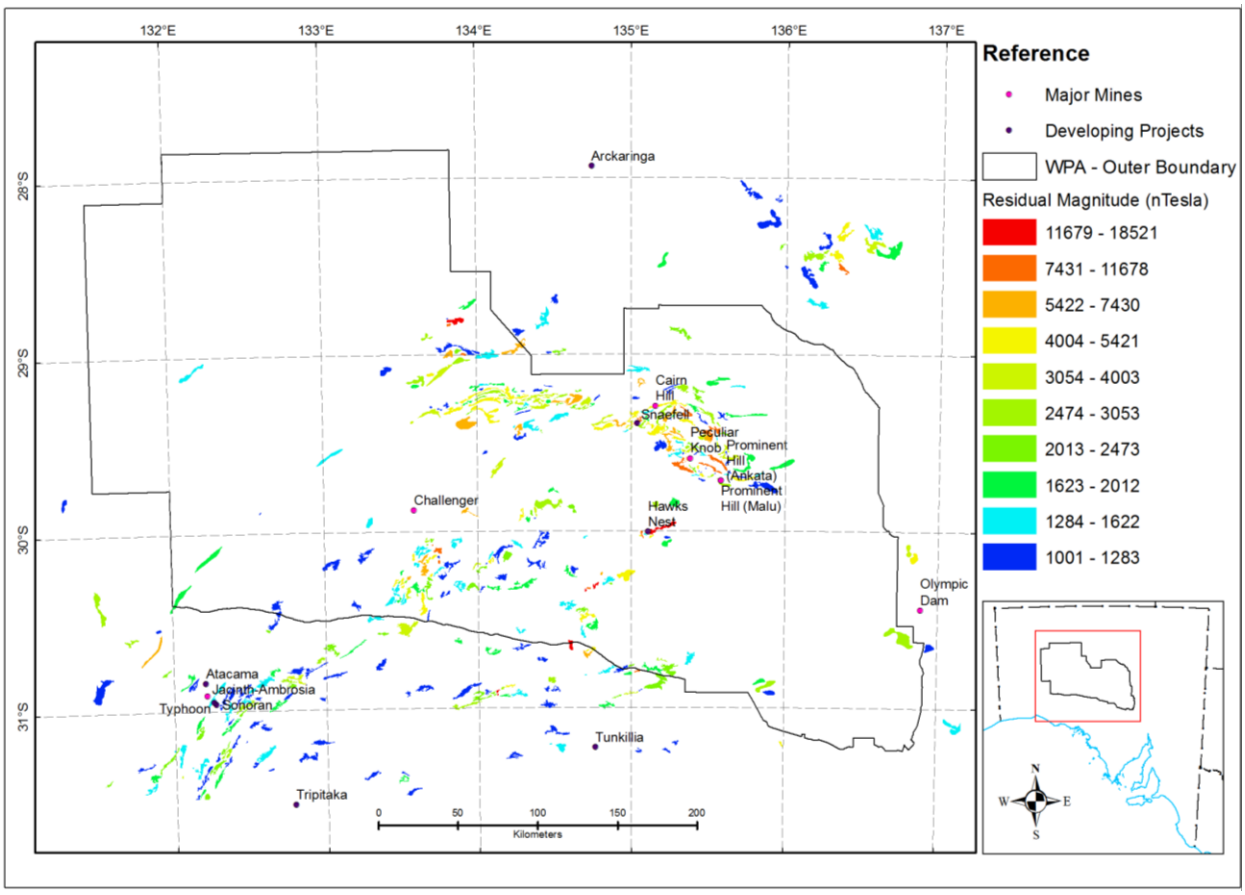

Figure 24. Filtered residual RTP TMI anomalies with a magnitude greater than 1000nT. The magnitude is the calculated difference between the contour value defining an anomaly and maximum value within the anomaly. (Plan number 205084-008)

The filtering illustrated in Figure 24 results in 437 features greater than 1000 nT. Unfiltered, there are 20,643 features. In this example, approximately 98% of anomalies have been filtered out of the results. This may be entirely appropriate for modelling a particular mineralisation style, while also providing a visual indication of clustering of high range magnetic features. Care should be taken when applying thresholds and filters, to avoid over-filtering.

Other attributes, including mean and standard deviation have been captured because the zonal statistics software produces them as part of the process. The utility of these additional attributes for analysis remains untested at this stage.

EXAMPLES OF HIGH VALUES IN THE GRAVITY DATASET

The gravity anomaly value ranges shown in Table 3 are given to display minimums and maximums of key attributes for the gravity anomaly polygon dataset. The highest gravity magnitude value coincides with known iron occurrences at Wilgena Hill iron ore deposit and the highest gravity maximum value coincides with a known iron occurrence at Peculiar Knob. High magnitude anomalies occurring at known deposits and prospects are evidence of the correlation between gravity anomalism and high density iron deposits, justifying the use of potential field data for mineral exploration and targeting. The attribution of the polygon data with anomaly magnitude enables selected value ranges of gravity anomaly magnitude to be the focus of targeting or mineral potential analysis. Additional high magnitude gravity features with no or little exploration history should be a focus for exploration.

CLUSTERING OF HIGH MAGNITUDE RESIDUAL GRAVITY ANOMALIES

The gravity anomaly dataset in Figure 10 was classified into 10 classes, using natural breaks. The classification suggests clustering of high magnitude anomalies in the Coober Pedy Ridge, Mabel Creek Ridge, Mount Woods Domain and Peake and Denison Inliers. These areas display high magnitude, broad gravity features in the gridded data, so clustering of the vectorised anomalies is expected. Nevertheless, the ability to demonstrate this using spatial statistics is an important first step in separating high magnitude clusters from outliers. The Getis-Ord General G statistic shown in Figure 14 confirmed statistically significant clustering of high gravity magnitude values occurring in the study area that are not the result of random chance and therefore warrant further investigation to understand any underlying geological explanations for the clustering.

The cluster and outlier analysis (Anselin Local Moran's I) maps high magnitude spatial clusters and outliers demonstrating a useful application of the tool because it indicated both the extent of gravity and magnetic intensity anomaly clusters and picked out statistical high magnitude outliers. Demonstrating that high magnitude anomalies occur in clusters and that outlier anomalies exist, has the potential to narrow the search for commodities for which a high magnitude potential field anomaly is preferred as a target, while drawing attention to features in areas where an anomaly is a statistical outlier.

In the study area, high clusters were highlighted in the Coober Pedy Ridge, Mabel Creek Ridge, Mount Woods Domain and Peake and Denison Inliers. The high clustering in these regions is thought to coincide with shallow (<150 m) basement and metamorphosed iron rich rocks.

High-low clusters (outliers, orange anomalies in Fig. 15) are evident in the east of the study area, almost exclusively in and around the Olympic Domain. These high-low clusters are of particular interest because they represent gravity highs among regions of low or insignificant gravity anomalies. Potentially, these high-low clusters could be explained by geological features such as hematite alteration systems, or alternatively dense rock bodies such as gabbro intruded into low metamorphic grade sediments or felsic volcanics. Alteration comprising pyroxene and garnet in skarn bodies could also account for density anomalies in this region. In general, the anomalies in the eastern portion of the study area are not as readily explained as the high clusters in the north and warrant further investigation. Many of the high-low anomalies within the Olympic Domain

coincide with known IOCG mines, deposits and prospects, displayed in Figure 25, suggesting that there are a number of additional, possible IOCG targets in the Olympic Domain. The distribution of the high-low outliers in and around the Olympic Domain indicates a possible re-delineation of the informal Olympic Subdomain (shown in Fig. 25), based on the nature of the gravity response.

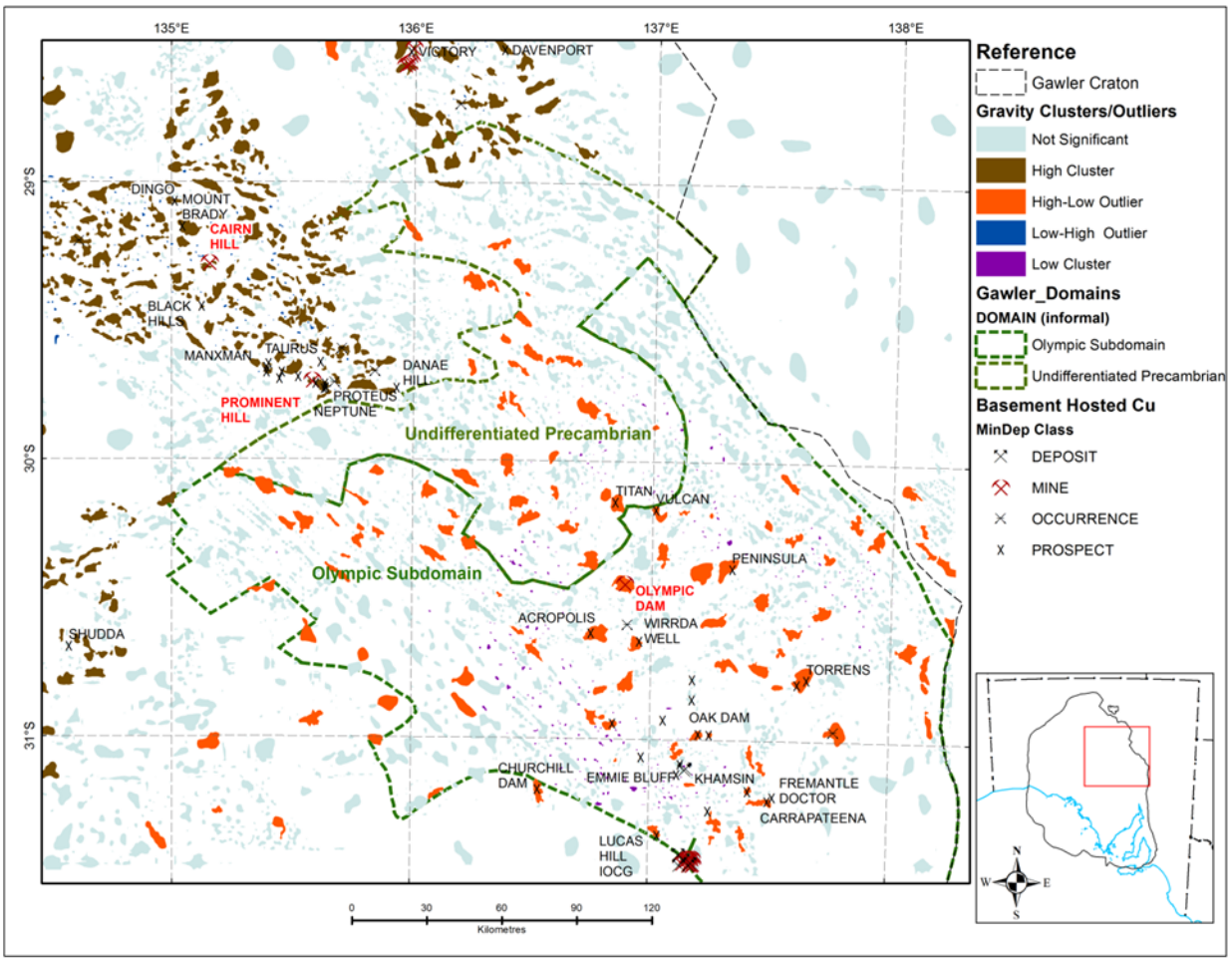

Figure 25. High-low clustering of gravity anomalies within the Olympic Domain coincide with known IOCG deposits and occurrences, including Olympic Dam. The green lines show the informal Olympic Subdomain and Undifferentiated Precambrian domain boundaries. (Plan number 205084-009)

EXAMPLES OF HIGH VALUES IN THE TMI DATASET

The value ranges shown in Table 4 were given to display minimums and maximums of key attributes for the TMI anomaly dataset. The Giffen Well Iron Ore deposit recorded both the highest magnitude and highest maximum residual TMI values. High magnitude TMI anomalies are almost certainly associated with magnetite and are key criteria in iron ore deposit targeting. As was the case with the gravity data, the utility of the classified magnetic anomaly data is in its ability to highlight data ranges that are prospective for a given commodity. This also allows ranking of anomaly data from high to low, which lends itself to mineral potential modelling.

CLUSTERING OF HIGH MAGNITUDE RESIDUAL TMI ANOMALIES

The RTP TMI anomaly dataset shown in Figure 16 displays a more closely spaced set of anomalies than observed in the gravity data. This is interpreted to be due primarily to the higher resolution of the TMI grid (line spacing of approximately 200–400 m, gridded at 35 m) when compared with the gravity grid (average station spacing of approximately 1000 m, gridded at 100 m). The higher resolution of TMI data acquisition captures subtle fluctuations in the magnetic property. The geometry of the TMI anomalies and associated contours is also more complex than that seen in the gravity data, necessitating different parameters when vectorising the data, when compared with gravity.

Like the gravity data, the TMI anomaly dataset displays characteristics of clustering of high values. High Range TMI anomalies (residual magnitudes >11,000 nT) in several parts of the study area coincide with known iron occurrences related to magnetite-rich banded iron formations. This is seen at Giffen Well and Kestrel deposits.

The high clusters and high-low clusters shown in Figure 19 occurred in Mabel Creek Ridge, Coober Pedy Ridge, Mount Woods Domain, Peake and Denison Inliers, Christie Domain, Wilgena Domain, Fowler Domain and the Harris Greenstone Belt. The data suggests these areas warrant attention, to determine possible explanations for the clusters and whether they have relevance for exploration targeting. Initial considerations include magnetite-rich lithologies, magnetite-quartzite, BIF, basalts, metasomatic Fe etc.

Unlike the gravity data, there were no low clusters in the TMI cluster and outlier analysis.

The association between magnetite and later hematite alteration within IOCG deposits is well documented (Direen and Lyons, 2007; Skirrow, 2008) and forms a basis for geophysical targeting of IOCG's in South Australia. Residual TMI anomaly magnitudes associated with known IOCG deposits and occurrences in and around Olympic Dam ranges from a few hundred to several thousand nT and are significantly lower in magnitude than those found in the west, in and around the Coober Pedy Ridge.

Thresholds applied to the TMI data have the capability to filter all but the desired range of magnitudes within the TMI data for application to mineral potential models, as shown in Figure 24. This is useful for testing hypotheses about ranges of values that are interpreted to be candidates for the style of mineralisation sought. To maximise the value of TMI data in IOCG modelling, it is necessary to understand and quantify the expression of TMI in and around hematite breccia-hosted IOCG systems to better utilise the magnetic anomaly data for exploration targeting. The data suggest that low to moderate magnetic anomalism is sufficient for a hematite-rich, breccia-hosted IOCG deposit, as illustrated in Figure 26, where Olympic Dam, Wirrda Well and other nearby prospects display moderate anomalism in the TMI data.

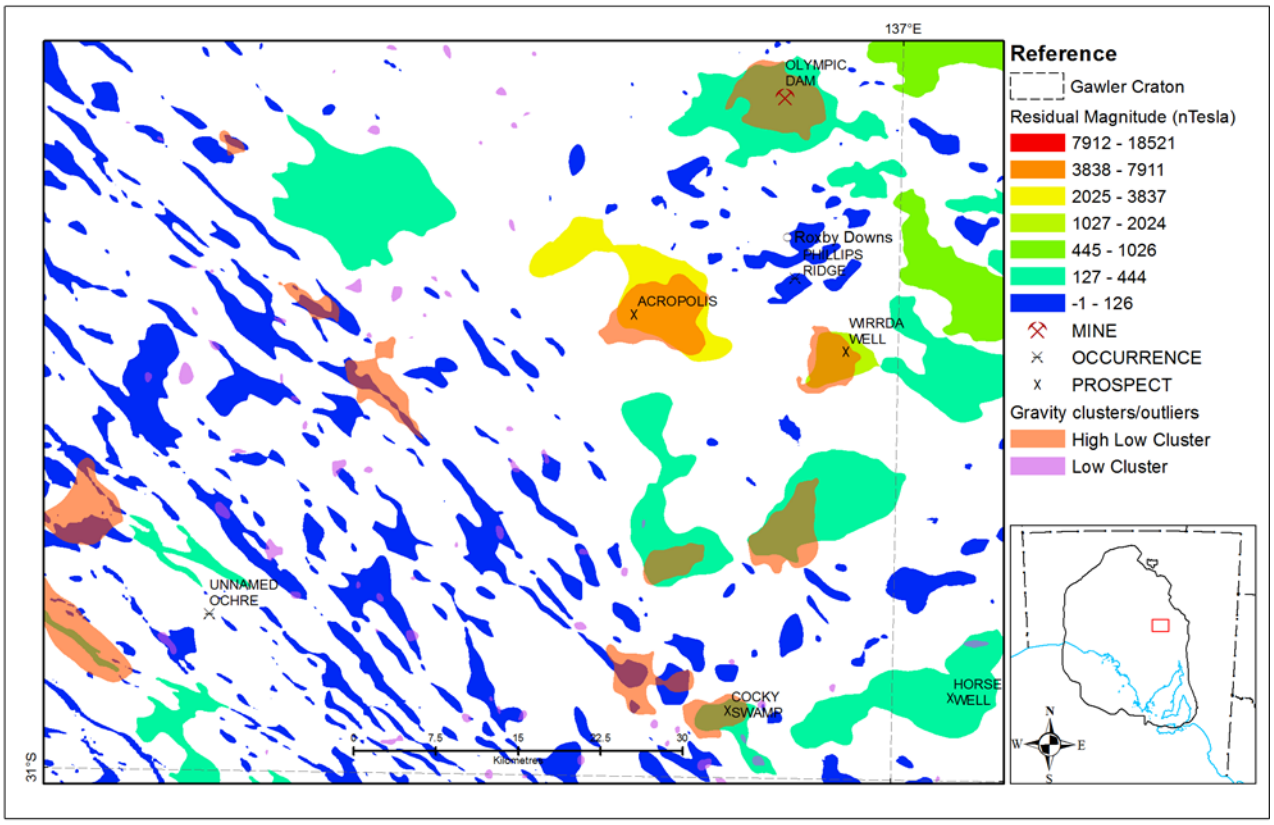

Figure 26. Low to moderate magnitude TMI anomalies in the Olympic domain coincident with high magnitude gravity anomalies in the Olympic Domain.

EVALUATING SPATIALLY COINCIDENT GRAVITY AND TMI ANOMALIES

Skirrow (2008) proposed criteria for recognising terranes with high IOCG potential to include the presence of hematite-rich zones laterally adjacent to or above magnetite-bearing zones. Hematite breccia hosted IOCGs in the northern Olympic Domain can and have been targeted on the assumption of geophysical signatures comprising a coincident (hematite-rich zone above a magnetite-bearing zone) or semi-coincident (hematite-rich zone lateral to a magnetite-bearing zone) gravity and magnetic anomalies.

Spatially coincident and semi-coincident gravity and magnetic anomalies generated by the process outlined in this report can be selected using GIS, based on their spatial separation distance. Examples are shown in Figures 21 and 22, which show coincident anomalies using separation distances of 1000 m and 100 m, respectively. Early trials of the technique discussed here found that many IOCG deposits and prospects were associated with a coincident gravity and magnetic anomaly, but the anomaly datasets show that there are thousands of such anomaly pairs within the study area. Further refinement of results using filtering, ranking of anomaly magnitude, outlier analysis or shape analysis and comparison with solid geology interpretations can be performed to minimise what may be considered to be false positives.

For example, the gravity high-low outliers highlighted by the cluster and outlier analysis within the TMI region appear in Figure 27, overlain by magnetic anomalies within 100 m of gravity features. This has reduced the search from many hundreds of geophysical targets to several dozen.

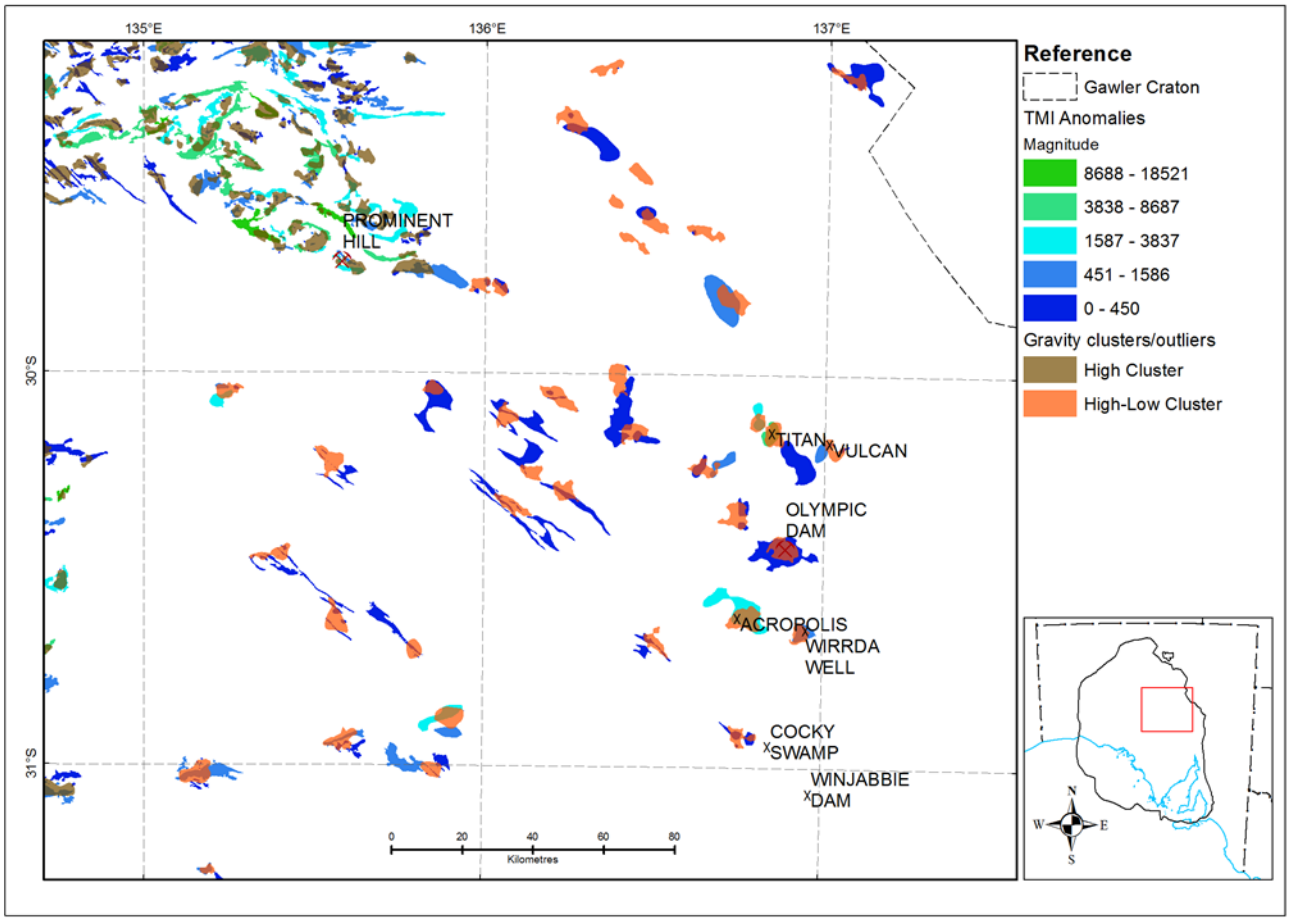

Figure 27. Low to moderate magnitude TMI anomalies in the Olympic domain coincident with high magnitude gravity anomalies in the Olympic Domain.

FUTURE WORK

As higher resolution gravity and magnetic data are produced for the entire Olympic Cu-Au Province, residual gravity and magnetic images and derived anomaly datasets will be appended to the current datasets.

The results given in this report will be incorporated into mineral potential maps of the region.

THE DATA PACKAGE

The data package released with this report is version 1.0. The data package will be updated as new gravity and TMI datasets become available and are reprocessed. Subsequent releases will be indicated by incremental version number changes.

ACKNOWLEDGEMENTS

The author would like to acknowledge the support of the Geological Survey of South Australia and reviewers of the report.

REFERENCES

Anselin L 1995. Local Indicators of Spatial Association—LISA. *Geographical Analysis* 27(2):93–115.

Budd AR and Skirrow RG 2007. The nature and origin of gold deposits of the Tarcoola goldfield and implications for the central Gawler gold province, South Australia. *Economic Geology* 102:1541–1563.

Chalmers NC 2007. *Mount Woods Domain: Proterozoic metasediments and intrusives*, Report Book 2007/20. Department State Development, South Australia.

Daly SJ, Fanning CM and Fairclough MC 1998. Tectonic evolution and exploration potential of the Gawler Craton, South Australia. *AGSO Journal of Australian Geology & Geophysics* 17:145–168.

de Smith MJ, Goodchild MF and Longley PA 2015. Geospatial Analysis. A Comprehensive Guide to Principles, Techniques and Software Tools. 5th Edition.

Direen NG and Lyons P 2007. Regional Crustal Setting of Iron Oxide Cu-Au Mineral Systems of the Olympic Dam Region, South Australia: Insights from Potential-Field Modeling. *Economic Geology* 102:1397–1414.

Drown CG 2003. The Barns Gold Project - discovery in an emerging district. *MESA Journal* 28:4–9. Department of Primary Industries and Resources South Australia, Adelaide.

ESRI 2013. ArcGIS Help 10.1., Cluster and Outlier Analysis (Anselin Local Moran's I) (Spatial Statistics) Online, http://resources.arcgis.com/en/help/main/10.1/index.html#//005p0000000z000000

Ferris GM and Schwarz MP 2003. Proterozoic gold province of the Central Gawler Craton. *MESA Journal* 30:4–12. Department of Primary Industries and Resources South Australia, Adelaide.

Ferris GM, Schwarz MP and Heithersay P 2002. The geological framework, distribution and controls of Fe-oxide and related alteration, and Cu-Au mineralisation in the Gawler Craton, South Australia. Part I: geological and tectonic framework. In TM Porter ed., *Hydrothermal iron oxide copper-gold and related deposits: a global perspective*. PGC Publishing, Adelaide, pp. 9–31.

Fraser AR, Reid A and Stern RA 2012. Timing of deformation and exhumation across the Karari Shear Zone, north-western Gawler Craton, South Australia. *Australian Journal of Earth Sciences* 59:547–570.

Fraser G and Lyons P 2006. Timing of Mesoproterozoic tectonic activity in the northwestern Gawler Craton constrained by $^{40}Ar/^{39}Ar$ geochronology. *Precambrian Research* 151:160–184.

Getis A and Ord JK 1992. The Analysis of Spatial Association by Use of Distance Statistics. *Geographical Analysis* 24(3):189–206.

Gupta VK and Ramani N 1980. Some aspects of regional-residual separation of gravity anomalies in a Precambrian terrain. *Geophysics* 45(9):1412–1426.

Hand M, Reid A and Jagodzinski E 2007. Tectonic framework and evolution of the Gawler Craton, South Australia. *Economic Geology* 102:1377–1395.

Hearst RB and Morris WA 2001. Case History. Regional gravity setting of the Sudbury Structure. *Geophysics* 66(6):1680–1690.

Howard KE 2011. Geotectonics in the Gawler Craton: Constraints from geochemistry, U-Pb geochronology and Sm-Nd and Lu-Hf isotopes. Unpublished PhD thesis, University of Adelaide.

Jagodzinski E and Reid AJ 2010. New zircon and monazite geochronology using SHRIMP and LA-ICPMS, from recent GOMA drilling, on samples from the northern Gawler Craton. In RJ Korsch and N Kositcin eds, *GOMA (Gawler Craton-Officer Basin-Musgrave Province-Amadeus Basin) Seismic and MT Workshop 2010*. Record, 2010/39, pp. 108–117. Geoscience Australia, Canberra.

Langenheim VE, Wright TL, Okaya DA, Yeats RS, Fuis GS, Thygesen K and Thybo H 2012. Structure of the San Fernando Valley region, California: Implications for seismic hazard and tectonic history. *Geosphere* 7(2):528–572.

Langenheim VE and Hildenbrand TG 1997. Commerce geophysical lineament - Its source, geometry, and relation to the Reelfoot rift and New Madrid seismic zone. *Geological Society of America Bulletin* 109(5):580–595.

Pilkington M and Cowan DR 2006. Model-based Separation Filtering of Magnetic Data. *Geophysics* 71(2):L17–L23.

Reid AJ and Hand M 2012. Mesoarchean to Mesoproterozoic evolution of the southern Gawler Craton, South Australia. *Episodes* 35:216–225.

Skirrow RG, Bastrakov E, Davidson G, Raymond OL and Heithersay P 2002. The geological framework, distribution and controls of Fe-oxide and related alteration, and Cu-Au mineralisation in the Gawler Craton, South Australia. Part II: Alteration and mineralisation. In TM Porter ed., *Hydrothermal iron oxide copper-gold and related deposits: a global perspective*. PGC Publishing, Adelaide, pp. 33–47.

Skirrow RG, Bastrakov EN, Barovich K, Fraser GL, Creaser RA, Fanning CM, Raymond OL and Davidson GJ 2007. Timing of iron oxide Cu-Au-(U) hydrothermal activity and Nd isotope constraints on metal sources in the Gawler Craton, South Australia. *Economic Geology* 102:1441–1470.

Skirrow RG 2008. 'Hematite-group' IOCG±U ore systems: Tectonic settings, hydrothermal characteristics, and Cu-Au and U mineralizing processes. In L Corriveau and H Mumin eds, *Exploring for Iron Oxide Copper-Gold Deposits: Canada and Global Analogues, Shortcourse Notes, GAC-MAC-SEG-SGA 2008, Quebec City, 29-30th May 2008*. Geological Association of Canada, in press.

Zeng H, Xu D and Tan H 2007. A model study for estimating optimum upward-continuation height for gravity separation with application to a Bouguer gravity anomaly over a mineral deposit, Jilin province, northeast China. *Geophysics* 72(4):145–150.

APPENDIXES

APPENDIX 1. DATA PACKAGE CONTENTS – GRID DATASETS

Gravity

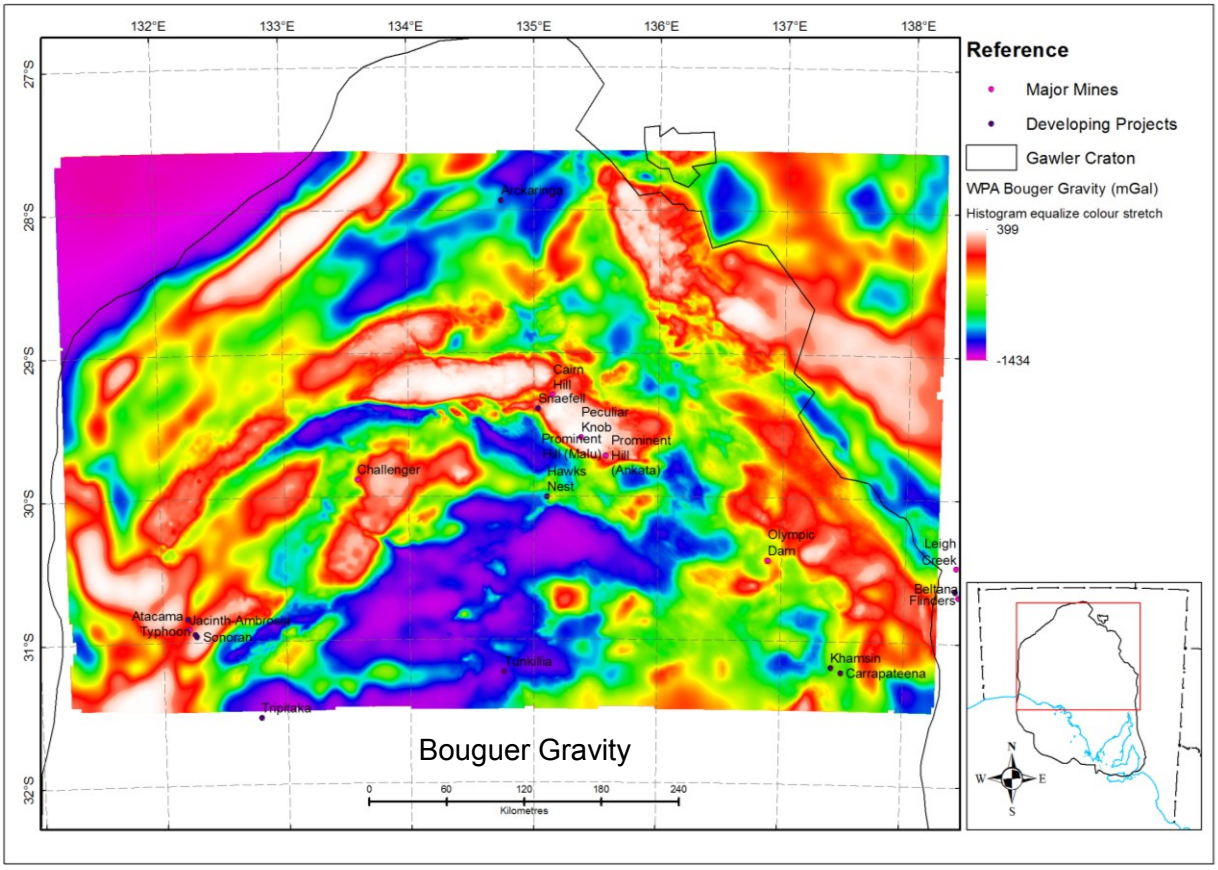

Bouguer Gravity

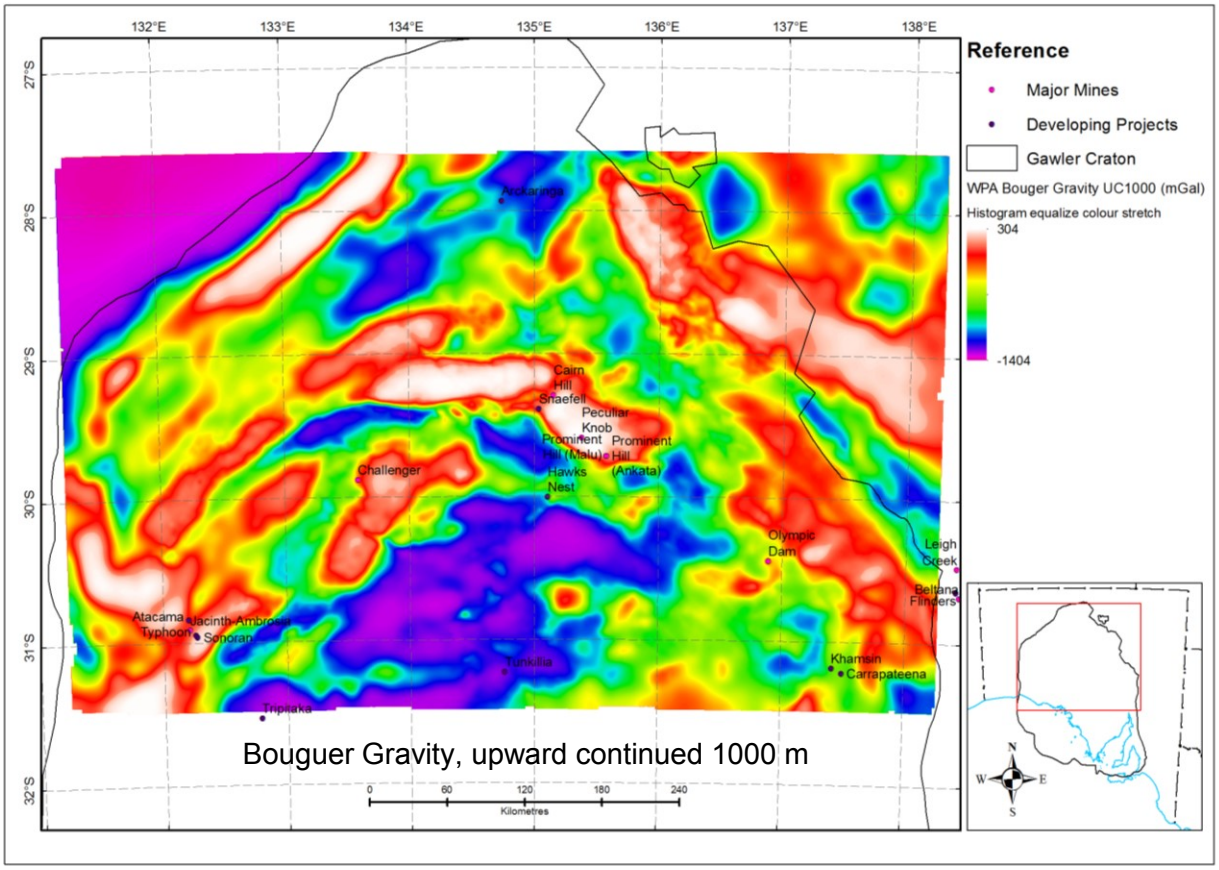

Bouguer Gravity, upward continued 1000 m

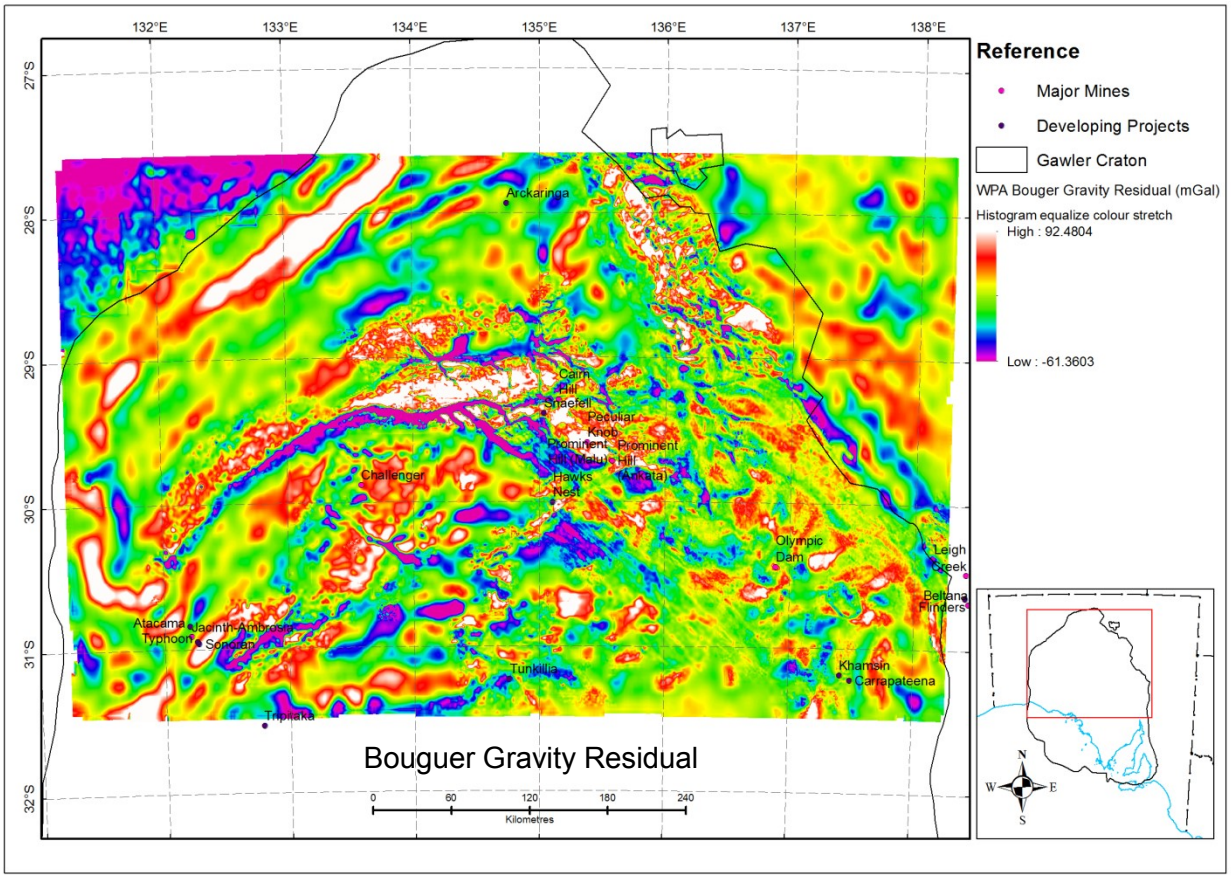
132°E
133°E
134°E
135°E
136°E
137°E
138°E
27°S
28°S
29°S
30°S
31°S
32°S
Reference
Major Mines
Developing Projects
Gawler Craton
WPA Bouger Gravity Residual (mGal)
Histogram equalize colour stretch
High : 92.4804
Low : -61.3603
Arckaringa
Cairn Hill
Snaefell
Peculiar Knob
Prominent Hill (Malu)
Prominent Hill (Ankata)
Challenger
Hawks Nest
Olympic Dam
Leigh Creek
Beltana
Flinders
Atacama
Jacinth-Ambrosia
Typhoon
Sonoran
Tunkillia
Khamsin
Carrapateena
Tripitaka
Bouguer Gravity Residual
0
60
120
180
240
Kilometres
N
W
E
S

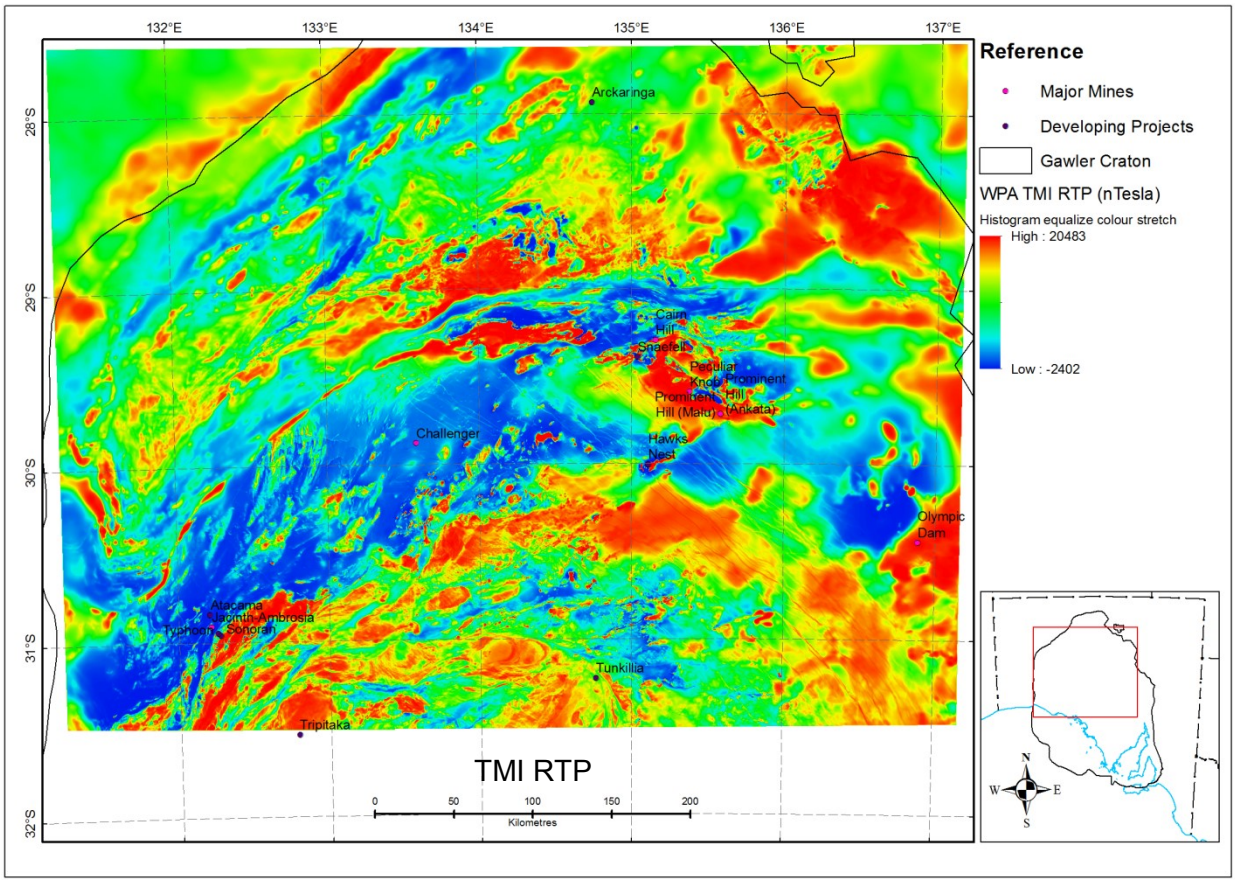
132°E
133°E
134°E
135°E
136°E
137°E
28°S
29°S
30°S
31°S
32°S
Reference
Major Mines
Developing Projects
Gawler Craton
WPA TMI RTP (nTesla)
Histogram equalize colour stretch
High : 20483
Low : -2402
Arckaringa
Cairn Hill
Snaefell
Peculiar Knob
Prominent Hill (Malu)
Prominent Hill (Ankata)
Challenger
Hawks Nest
Olympic Dam
Atacama
Jacinth-Ambrosia
Typhoon
Sonoran
Tunkillia
Tripitaka
TMI RTP
0
50
100
150
200
Kilometres
N
W
E
S

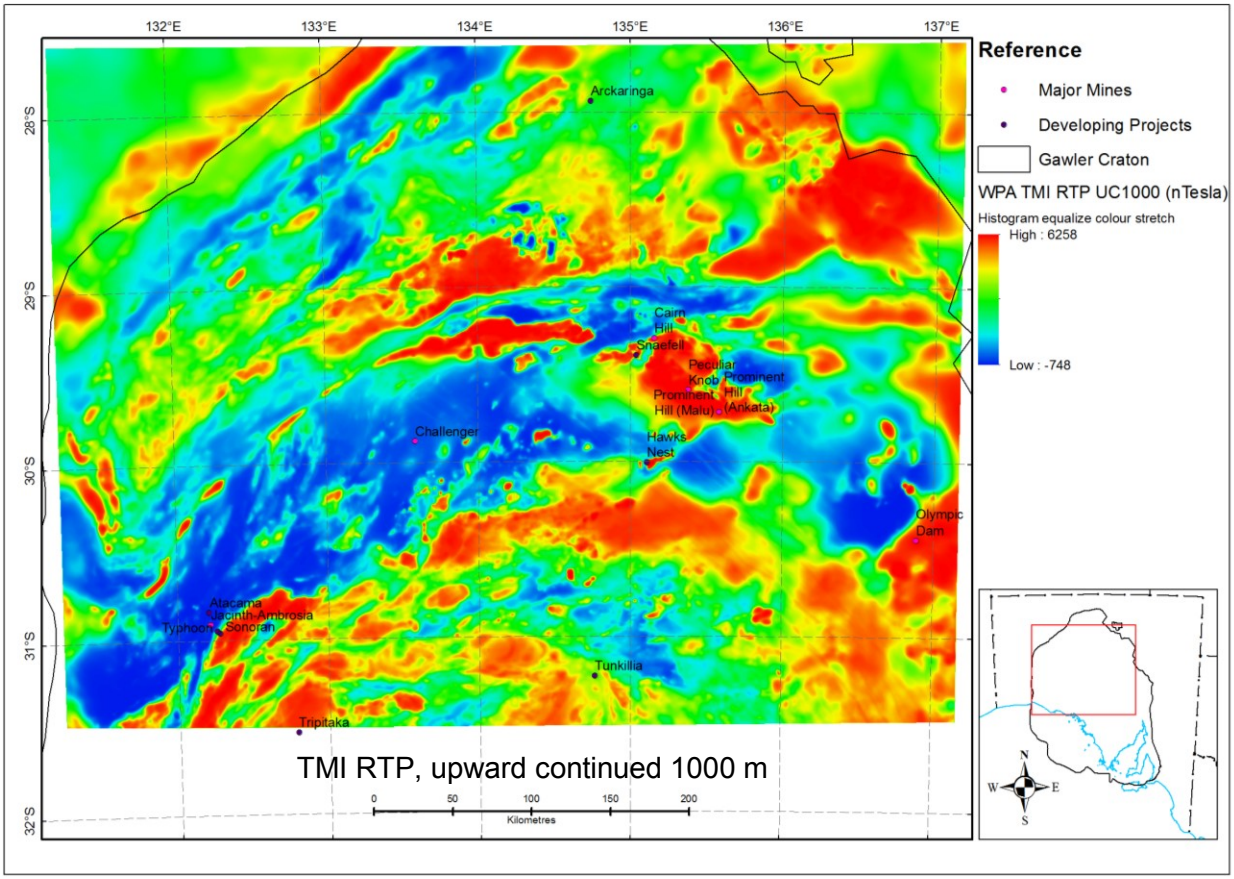

TMI RTP, upward continued 1000 m

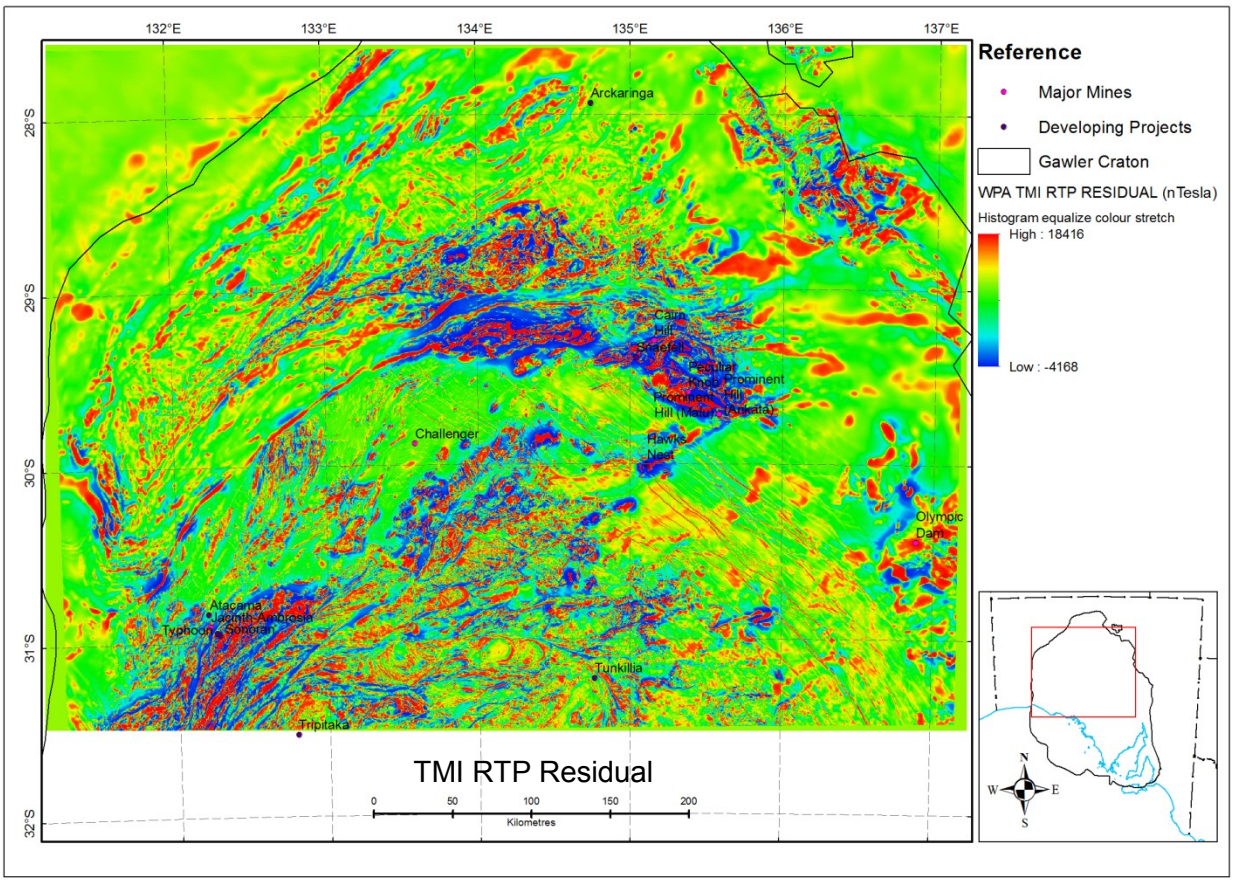

TMI RTP Residual

Grid statistics

Band Statistics	
Bouguer Gravity	
Min	-1434.227416992188
Max	399.0217590332031
Mean	-216.5457544656014
Std Deviation	236.9330997785909
Bouguer Gravity upward continued 1000 m	
Min	-1404.233764648438
Max	303.7150268554688
Mean	-216.7033252102032
Std Deviation	230.1737326280347
Residual Gravity	
Min	-62.798156738281
Max	97.839385986328
Mean	0.15757074443341
Std Deviation	10.832519210141
TMI RTP	
Min	-2652.561279296875
Max	21249.73046875
Mean	29.34306469116081
Std Deviation	452.9806745574223
TMI RTP upward continued 1000 m	
Min	-750.4716186523438
Max	6419.88330078125
Mean	29.6352473198239
Std Deviation	344.0160841926804
Residual TMI	
Min	-4168.1064453125
Max	18415.9296875
Mean	-0.2921826110892986
Std Deviation	194.3516046115218

APPENDIX 2. DATA PACKAGE CONTENTS – VECTOR DATASETS

Gravity

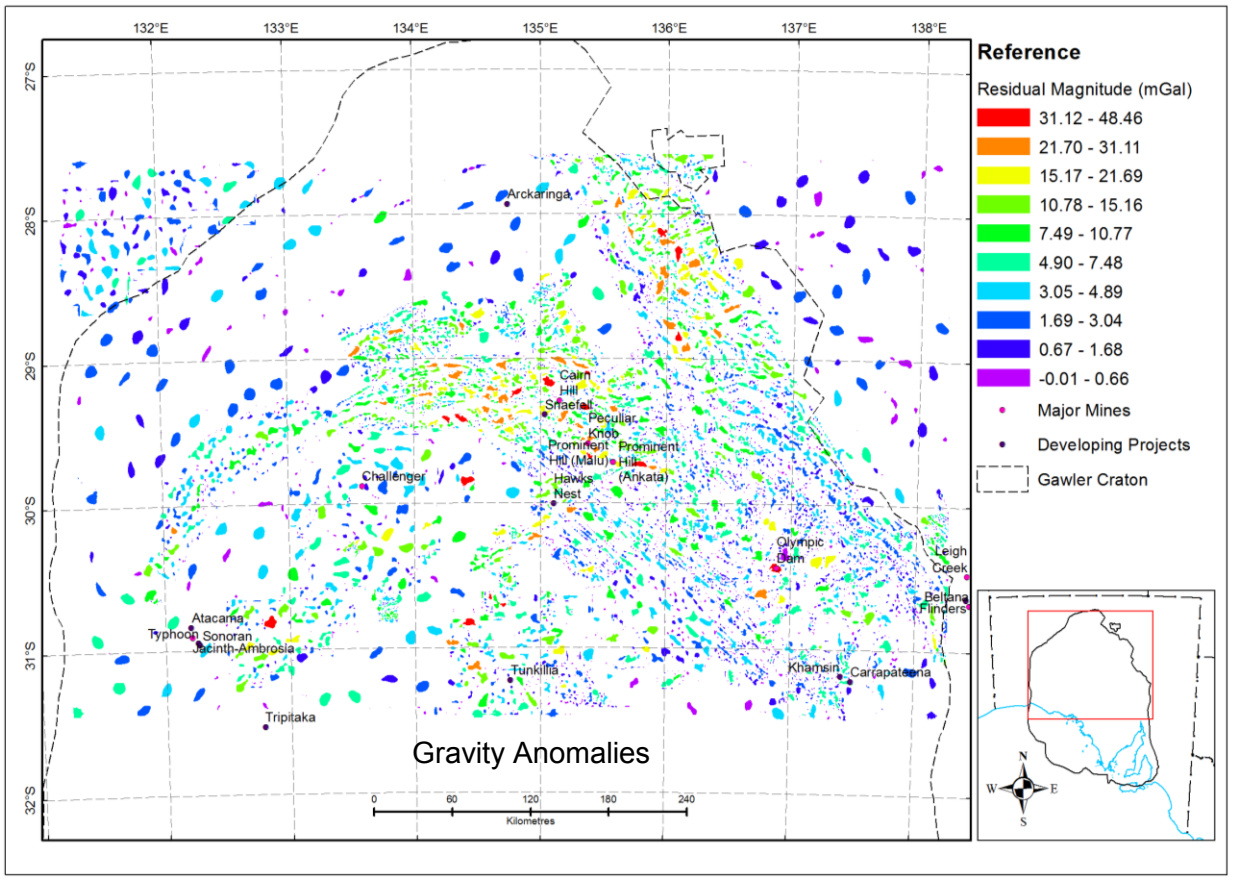

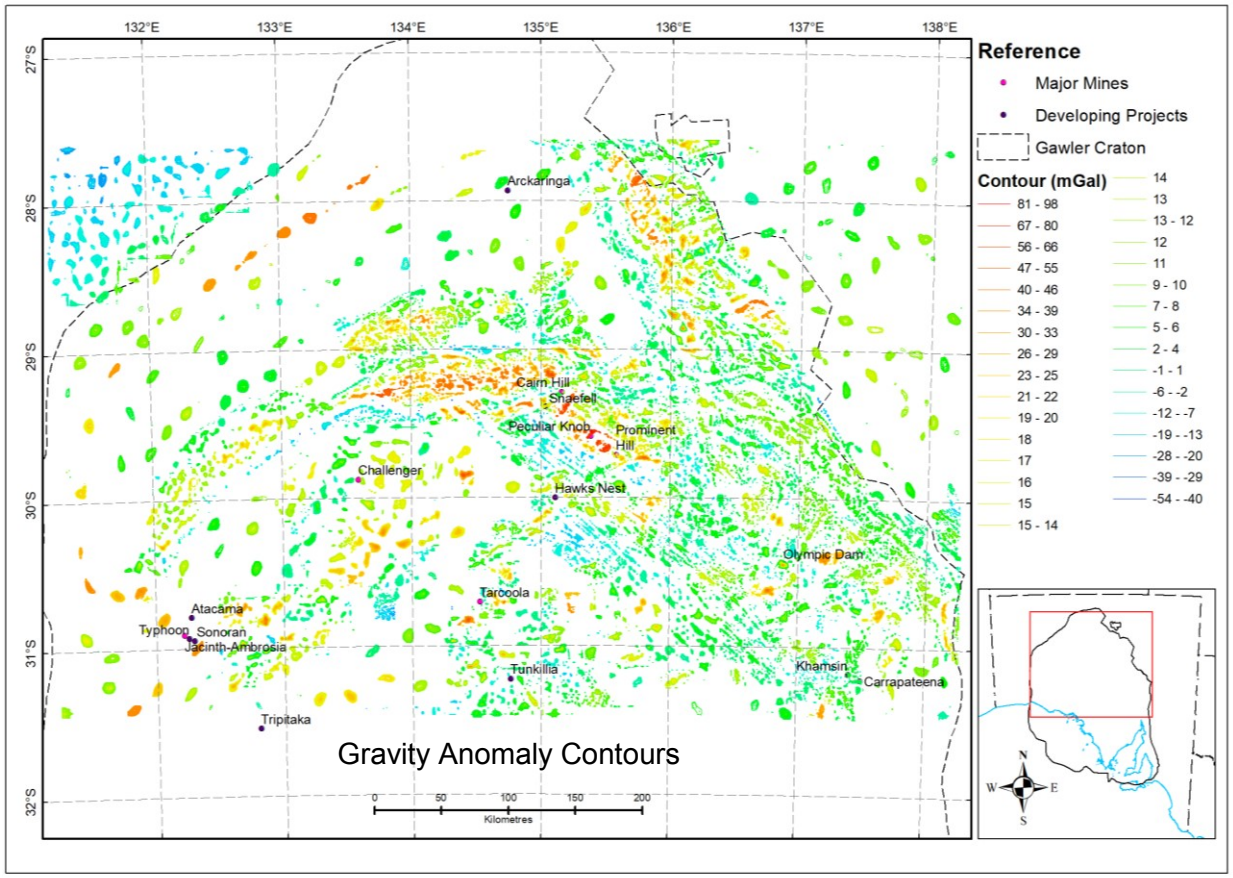

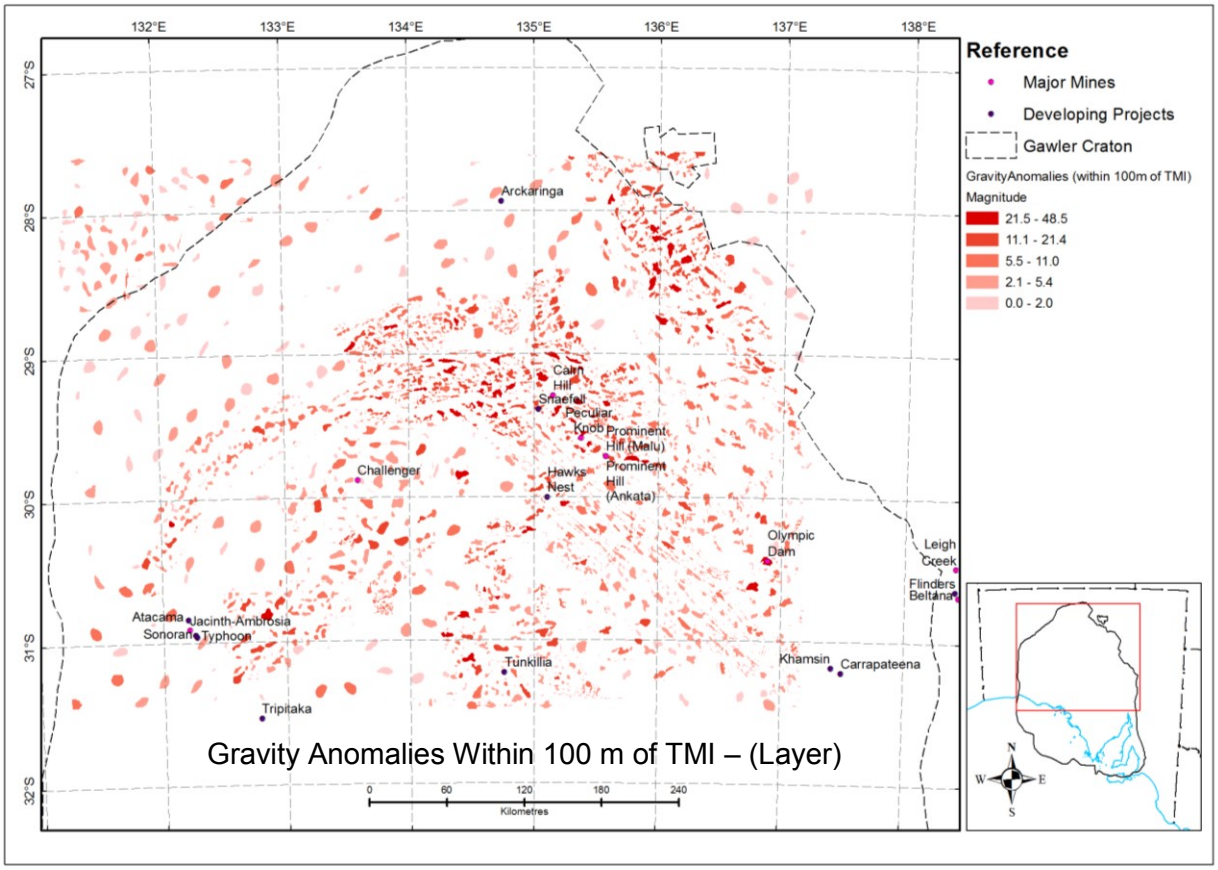

Gravity Anomalies Within 100 m of TMI – (Layer)

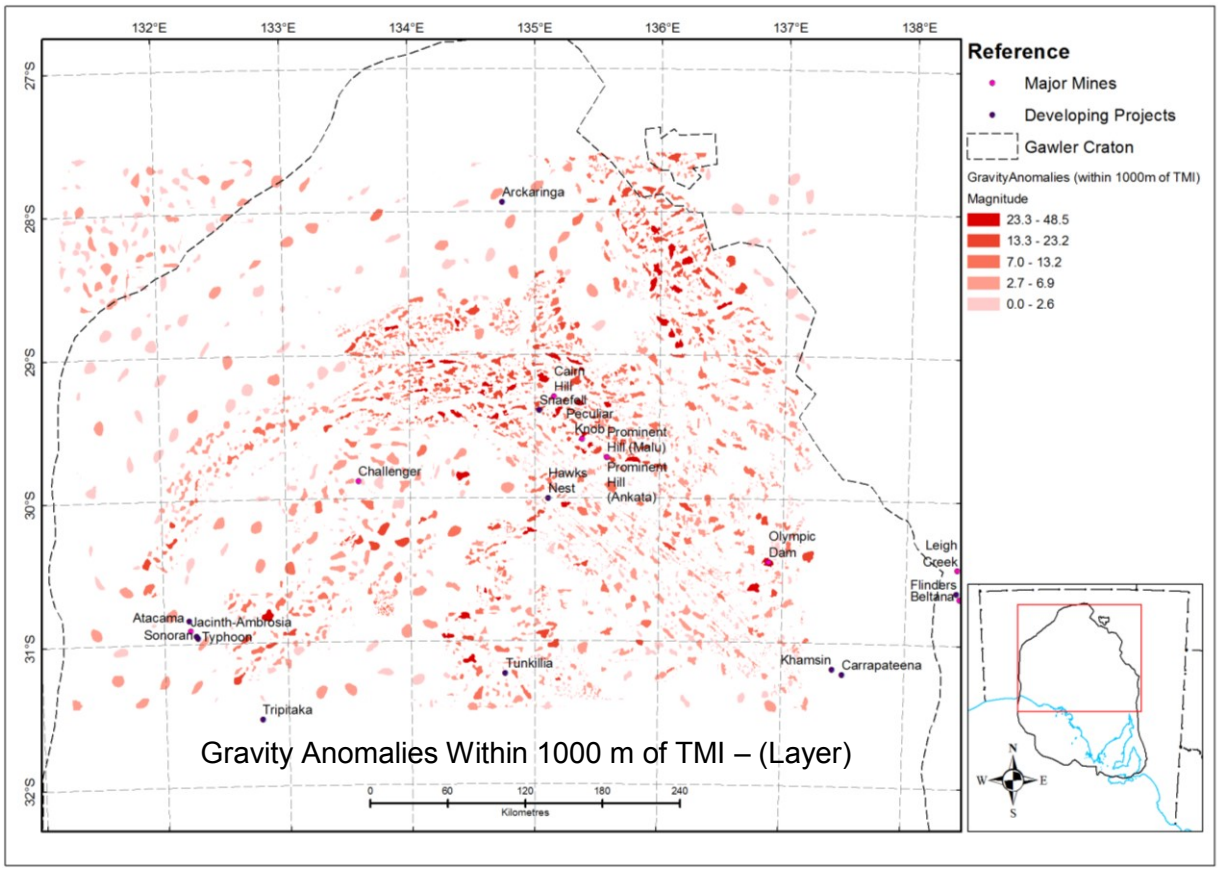

Gravity Anomalies Within 1000 m of TMI – (Layer)

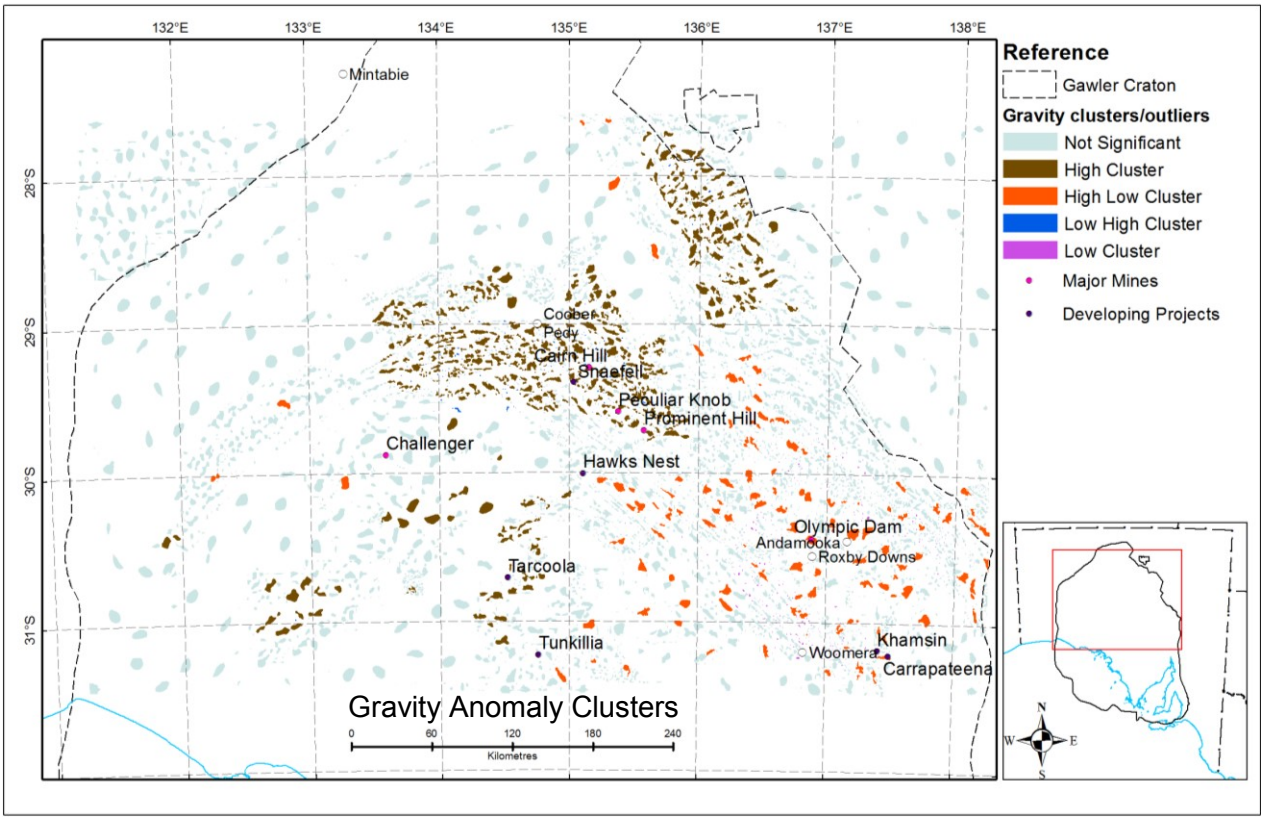
132°E
133°E
134°E
135°E
136°E
137°E
138°E
28°S
29°S
30°S
31°S
Mintabie
Coober Pedy
Cairn Hill
Snaefell
Peculiar Knob
Prominent Hill
Challenger
Hawks Nest
Olympic Dam
Andamooka
Roxby Downs
Tarcoola
Tunkillia
Woomera
Khamsin
Carrapateena
Gravity Anomaly Clusters
0 60 120 180 240
Kilometres
Reference
Gawler Craton
Gravity clusters/outliers
Not Significant
High Cluster
High Low Cluster
Low High Cluster
Low Cluster
Major Mines
Developing Projects
N
W
E
S

TMI

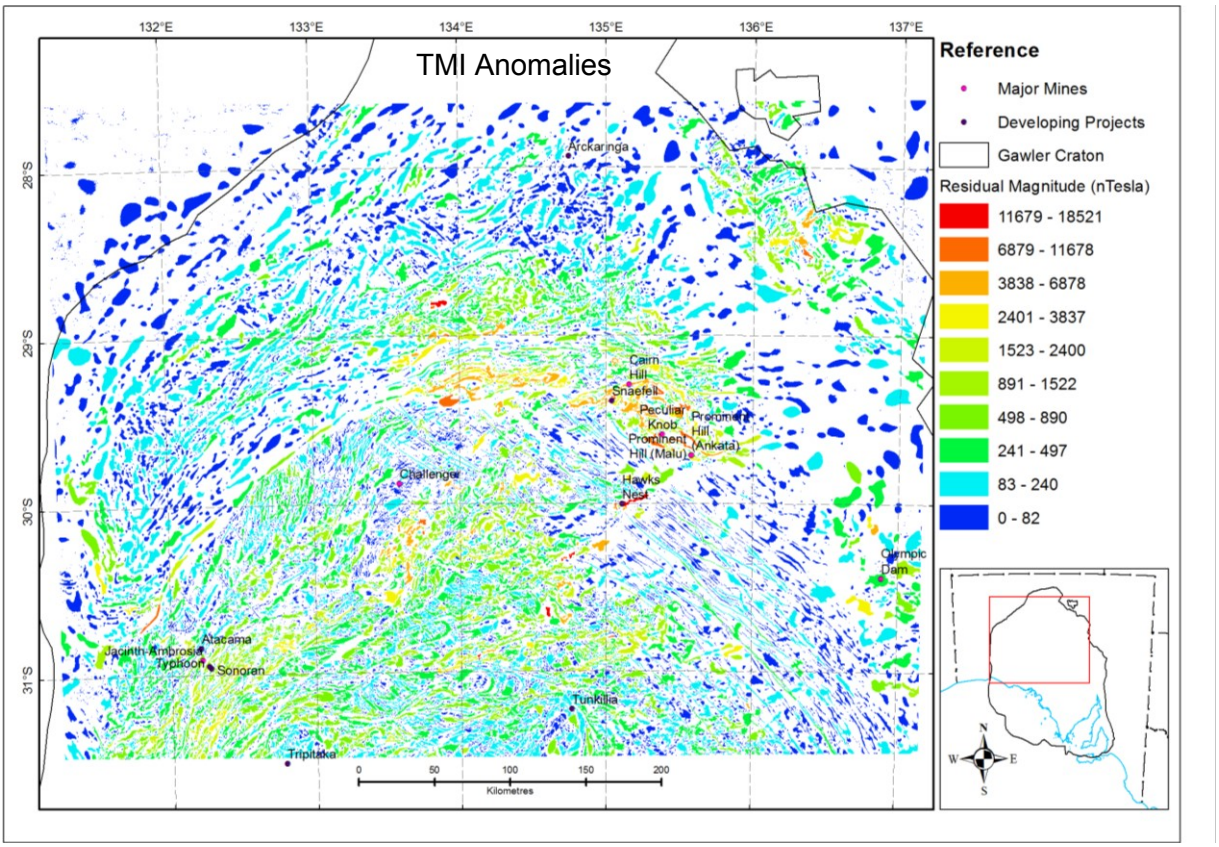
132°E
133°E
134°E
135°E
136°E
137°E
28°S
29°S
30°S
31°S
TMI Anomalies
Arckaringa
Cairn Hill
Snaefell
Peculiar Knob
Prominent Hill (Malu)
Prominent Hill (Ankata)
Challenger
Hawks Nest
Olympic Dam
Jacinth Ambrosia
Typhoon
Atacama
Sonoren
Tunkillia
Tripitaka
0 50 100 150 200
Kilometres
Reference
Major Mines
Developing Projects
Gawler Craton
Residual Magnitude (nTesla)
11679 - 18521
6879 - 11678
3838 - 6878
2401 - 3837
1523 - 2400
891 - 1522
498 - 890
241 - 497
83 - 240
0 - 82
N
W
E
S

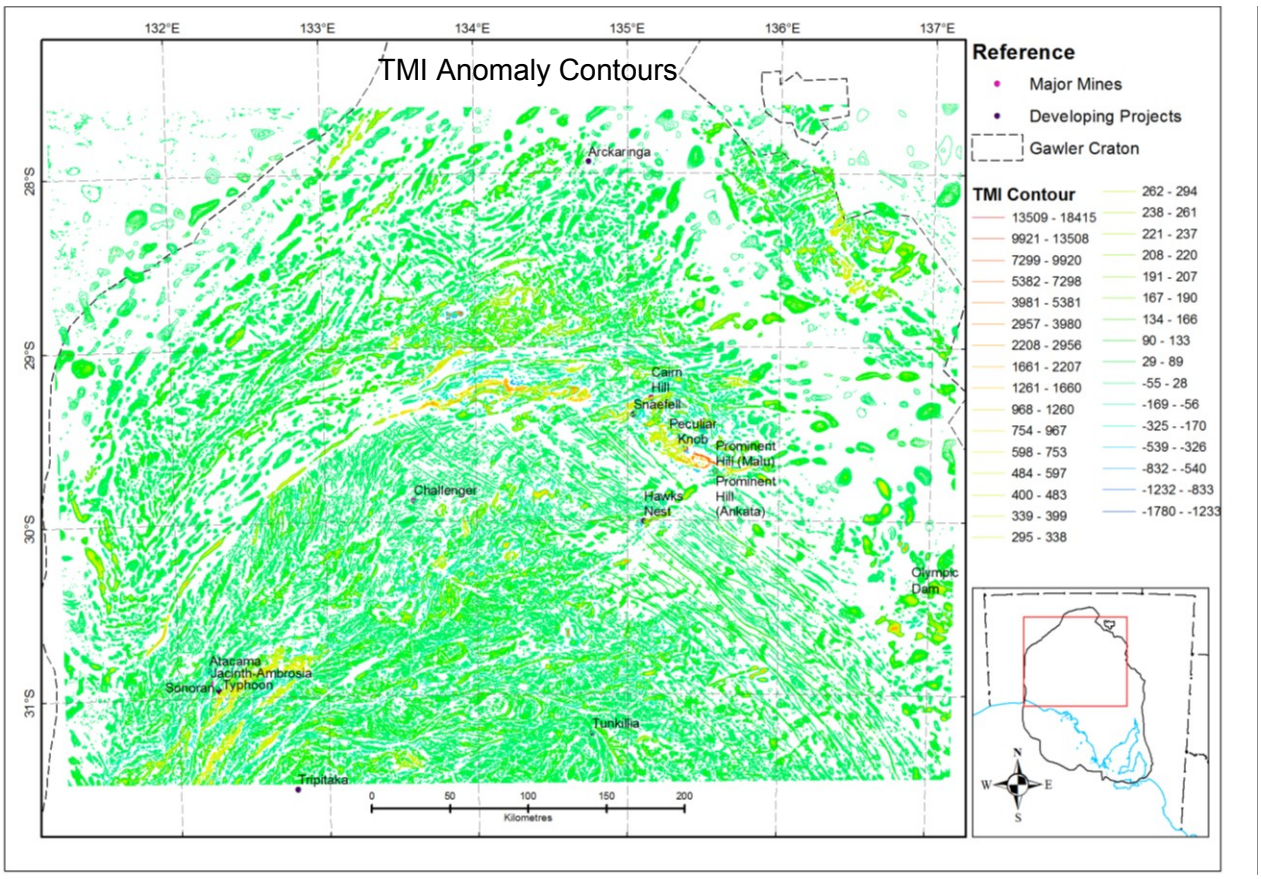
TMI Anomaly Contours
132°E
133°E
134°E
135°E
136°E
137°E
28°S
29°S
30°S
31°S
Arckaringa
Cairn Hill
Snaefell
Peculiar Knob
Prominent Hill (Malu)
Prominent Hill (Ankata)
Challenger
Hawks Nest
Olympic Dam
Atacama
Jacinth-Ambrosia
Sonoran
Typhoon
Tunkillia
Tripitaka
0
50
100
150
200
Kilometres
Reference
Major Mines
Developing Projects
Gawler Craton
TMI Contour
13509 - 18415
9921 - 13508
7299 - 9920
5382 - 7298
3981 - 5381
2957 - 3980
2208 - 2956
1661 - 2207
1261 - 1660
968 - 1260
754 - 967
598 - 753
484 - 597
400 - 483
339 - 399
295 - 338
262 - 294
238 - 261
221 - 237
208 - 220
191 - 207
167 - 190
134 - 166
90 - 133
29 - 89
-55 - 28
-169 - -56
-325 - -170
-539 - -326
-832 - -540
-1232 - -833
-1780 - -1233
N
W
E
S

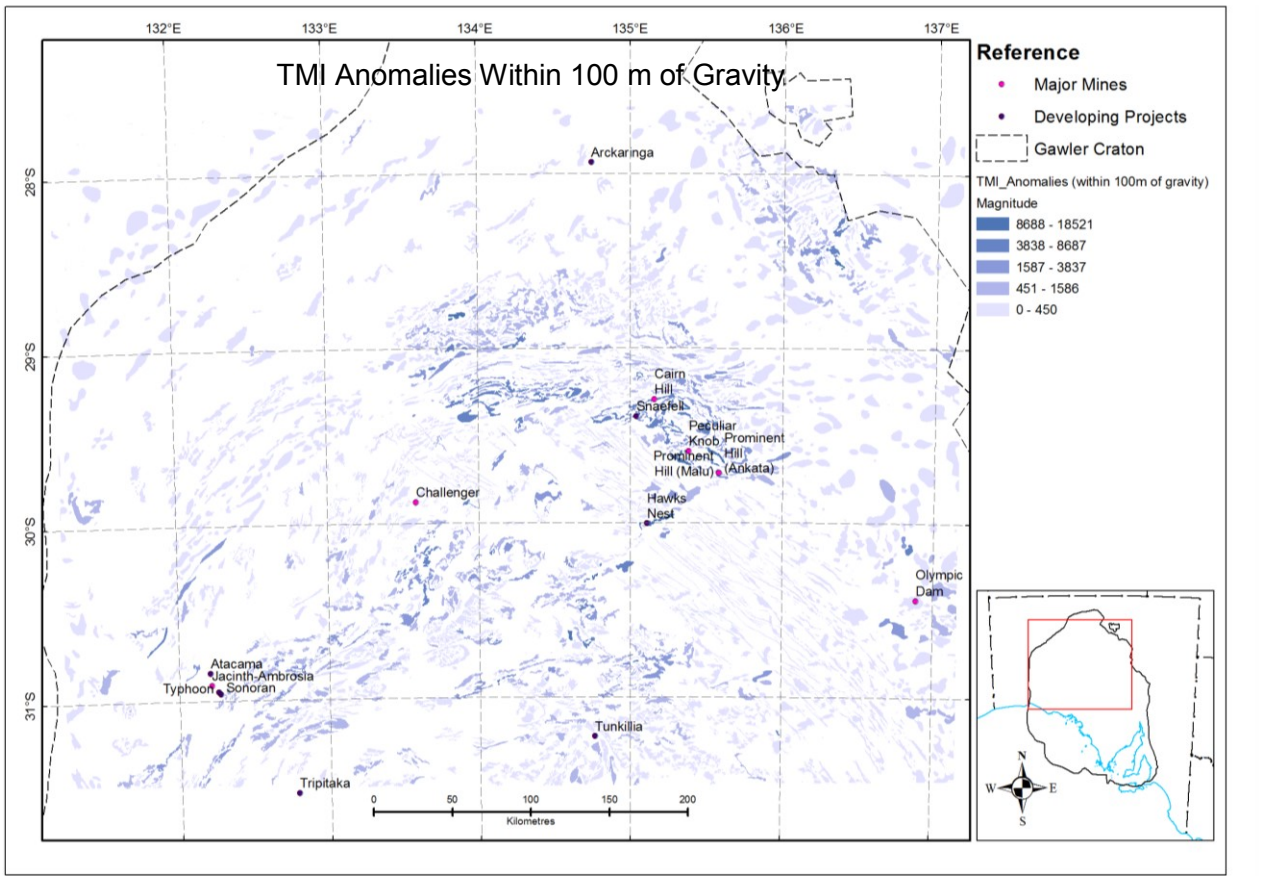
TMI Anomalies Within 100 m of Gravity
132°E
133°E
134°E
135°E
136°E
137°E
28°S
29°S
30°S
31°S
Arckaringa
Cairn Hill
Snaefell
Peculiar Knob
Prominent Hill (Malu)
Prominent Hill (Ankata)
Challenger
Hawks Nest
Olympic Dam
Atacama
Jacinth-Ambrosia
Typhoon
Sonoran
Tunkillia
Tripitaka
0
50
100
150
200
Kilometres
Reference
Major Mines
Developing Projects
Gawler Craton
TMI_Anomalies (within 100m of gravity)
Magnitude
8688 - 18521
3838 - 8687
1587 - 3837
451 - 1586
0 - 450
N
W
E
S

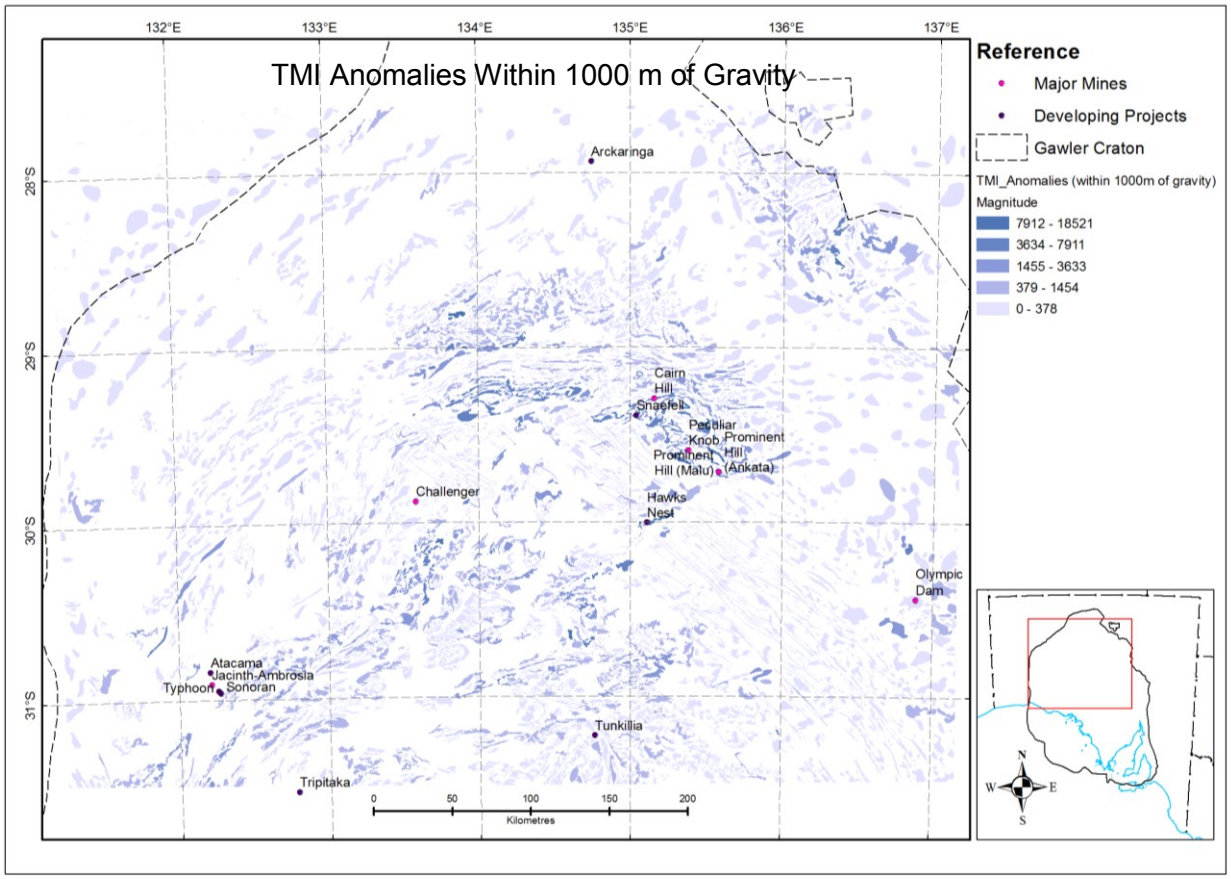
TMI Anomalies Within 1000 m of Gravity
132°E
133°E
134°E
135°E
136°E
137°E
28°S
29°S
30°S
31°S
Arckaringa
Cairn Hill
Snaefell
Peculiar Knob
Prominent Hill
Prominent Hill (Malu)
Hill (Ankata)
Challenger
Hawks Nest
Olympic Dam
Atacama
Jacinth-Ambrosia
Typhoon
Sonoran
Tunkillia
Tripitaka
0
50
100
150
200
Kilometres
Reference
Major Mines
Developing Projects
Gawler Craton
TMI_Anomalies (within 1000m of gravity)
Magnitude
7912 - 18521
3634 - 7911
1455 - 3633
379 - 1454
0 - 378
N
W
E
S

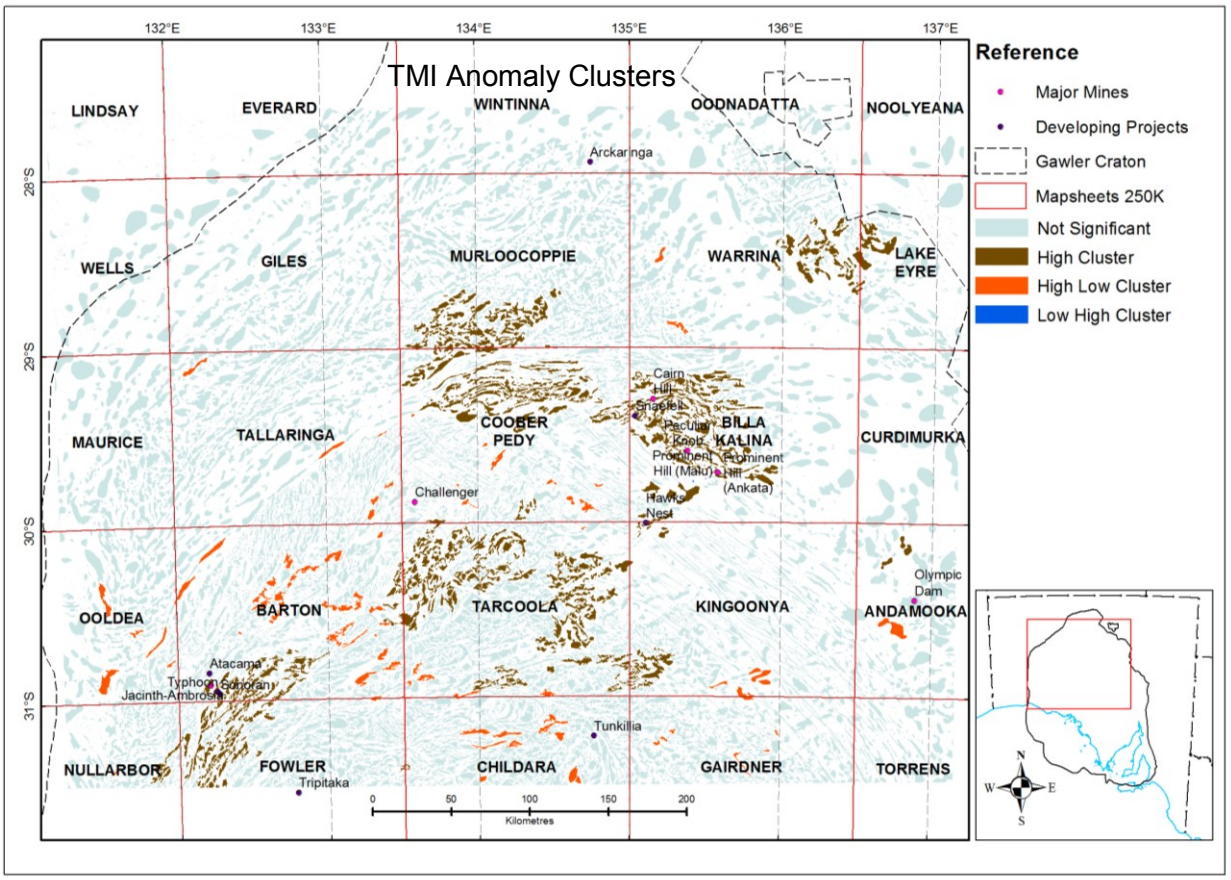
TMI Anomaly Clusters
132°E
133°E
134°E
135°E
136°E
137°E
28°S
29°S
30°S
31°S
LINDSAY
EVERARD
WINTINNA
OODNADATTA
NOOLYEANA
Arckaringa
WELLS
GILES
MURLOOCOPPIE
WARRINA
LAKE EYRE
MAURICE
TALLARINGA
COOPER PEDY
BILLA KALINA
CURDIMURKA
Cairn Hill
Snaefell
Peculiar Knob
Prominent Hill
Prominent Hill (Malu)
Hill (Ankata)
Challenger
Hawks Nest
OOLDEA
BARTON
TARCOOLA
KINGOONYA
ANDAMOOKA
Olympic Dam
Atacama
Typhoon
Sonoran
Jacinth-Ambrosia
Tunkillia
NULLARBOR
FOWLER
CHILDARA
GAIRDNER
TORRENS
Tripitaka
0
50
100
150
200
Kilometres
Reference
Major Mines
Developing Projects
Gawler Craton
Mapsheets 250K
Not Significant
High Cluster
High Low Cluster
Low High Cluster
N
W
E
S

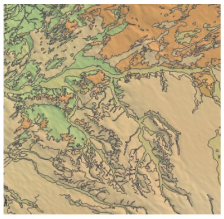

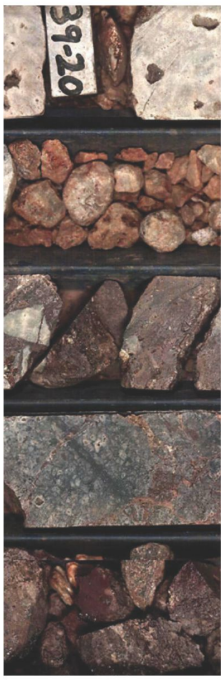

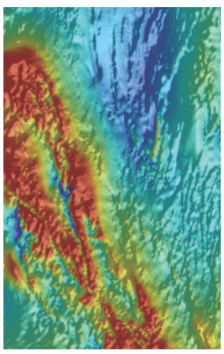

Department of State Development

Metadata: Exploration Targeting Using Residual Gravity and TMI Processed For GIS Analysis - Data Package

Date Printed: 11/07/2018

Government of South Australia

Department of State Development

Dataset

Title: Exploration Targeting Using Residual Gravity and TMI Processed For GIS Analysis - Data Package

Custodian: Department of Energy and Minerals

Jurisdiction: South Australia

Description

Abstract:
Gravity and reduced-to-pole total magnetic intensity grids over the northern Gawler Craton have been vectorised, generating polygon datasets representing regions of locally anomalous gravity and magnetic intensity. Statistics from potential field grids were embedded into each polygon which enabled calculation of anomaly magnitude. Analysis of spatial clustering and the identification of outliers using Anselin Local Morans I (ESRI 2013) has resulted in the delineation of geographic regions across the study area that exhibit either high magnitude clusters or high magnitude outliers, which correspond to known regional geological and metamorphic domains. Contours of residual gravity and TMI have also been provided in the data package, along with the grids that were used to generate the polygons and contours.

ANZLIC Search Terms:
GEOSCIENCES Geophysics
MINERALS

GEN Category: Woomera Prohibited Area

GEN Custodial Jurisdiction: Australia

GEN Name: South Australia

Geographic Extent Polygon: -27.62, 137.162, -31.523, 131.232

North bounding latitude: -27.62

South bounding latitude: -31.523

East bounding longitude: 137.162

West bounding longitude: 131.232

Data Currency

Beginning Date: 2013-08-14

End Date: 2015-07-02

Dataset Status

Progress: Complete

Maintenance: Not Planned

Version Number: 1

Access
Stored format: DIGITAL

Available format(s): DIGITAL

SARIG Layer(s): Geophysical State Images/Woomera Prohibited Area (WPA)/WPA TMI; WPA Gravity

Data Quality
Lineage: WPA Gravity and WPA TMI

Positional accuracy: Not Known

Attribute accuracy: Accurate for the purposes of analysis

Logical consistency: Consistent

Completeness: Complete

Contact Information
Contact organisation: Department of Energy and Mining

Contact position: Customer Service Centre

Contact mail address: GPO Box 320, Adelaide SA 5001

Contact telephone: 08 8463 3000

Contact email: resources.customerservices@sa.gov.au

Metadata Dates
Add date: 2018-06-21

Change date: 2018-07-11

Responsible Party
Responsible party: Geological Survey of South Australia

Responsible party function: Content provider

Description
Dataset classification: Derived

Spatial representation type: Vector:Polygon

Dimension: x,y

Usage

Purpose: This data is designed as an aid to geological and geophysical exploration.

Use: Used to supply industry, government and the general public with geophysical information, primarily used for mineral exploration and mapping.

Usage limitations: Designed for regional scale analysis and display, WPA_TMI is a combination of grids from various eras, instruments and companies; has not been further QC'd by Minerals Resources staff and may contain unexpected errors. Input data was gridded at cell sizes ranging from 10 metres to 1600 metres and the merged grid was gridded at 35m cell size. Interpretations should consider the variability of the input data. Gravity Grid was compiled from Gravity stations at intervals from 100m to 11,000m.

Dataset Associations

Origin

Dataset size: 4.6Gb

Projection: Other Lambert for South Australia

Datum: GDA94

Dataset Management

Authorised date: 2018-06-21

Authorised by: Mineral Resources Division

Attributes